1986-12

Development, validation and use of a computer-controlled system for the investigation of phase and amplitude shaded acoustic arrays

Butler, John D.

NAVAL POSTGRADUATE SCHOOL
Monterey, California

THESIS

DEVELOPMENT, VALIDATION AND USE OF A
COMPUTER-CONTROLLED SYSTEM FOR THE INVESTIGATION
OF PHASE AND AMPLITUDE SHADED ACOUSTIC ARRAYS

by

John Dale Butler

December 1986

Co-Advisors: A.B. Coppens
G.B. Netzorg

Approved for public release; distribution is unlimited.

SECURITY CLASSIFICATION OF THIS PAGE

REPORT DOCUMENTATION PAGE

1a REPORT SECURITY CLASSIFICATION: Unclassified	1b RESTRICTIVE MARKINGS
2a SECURITY CLASSIFICATION AUTHORITY	3 DISTRIBUTION/AVAILABILITY OF REPORT: Approved for public release; distribution is unlimited
2b DECLASSIFICATION/DOWNGRADING SCHEDULE	
4 PERFORMING ORGANIZATION REPORT NUMBER(S)	5 MONITORING ORGANIZATION REPORT NUMBER(S)
6a NAME OF PERFORMING ORGANIZATION: Naval Postgraduate School; 6b OFFICE SYMBOL (If applicable): 61	7a NAME OF MONITORING ORGANIZATION: Naval Postgraduate School
6c ADDRESS (City, State, and ZIP Code): Monterey, CA 93943-5000	7b ADDRESS (City, State, and ZIP Code): Monterey, CA 93943-5000
8a NAME OF FUNDING/SPONSORING ORGANIZATION; 8b OFFICE SYMBOL (If applicable)	9 PROCUREMENT INSTRUMENT IDENTIFICATION NUMBER
8c ADDRESS (City, State, and ZIP Code)	10 SOURCE OF FUNDING NUMBERS: PROGRAM ELEMENT NO; PROJECT NO; TASK NO; WORK UNIT ACCESSION NO

11 TITLE (Include Security Classification)
DEVELOPMENT, VALIDATION AND USE OF A COMPUTER-CONTROLLED SYSTEM FOR THE INVESTIGATION OF PHASE AND AMPLITUDE SHADED ACOUSTIC ARRAYS

12 PERSONAL AUTHOR(S)
Butler, John D.

13a TYPE OF REPORT	13b TIME COVERED	14 DATE OF REPORT (Year Month Day)	15 PAGE COUNT
Master's Thesis	FROM ____ TO ____	1986 December	94

16 SUPPLEMENTARY NOTATION

17 COSATI CODES			18 SUBJECT TERMS (Continue on reverse if necessary and identify by block number)
FIELD	GROUP	SUB-GROUP	Computer-controlled testing, Phase Shaded Array, Amplitude Shaded Array, Beam Pattern Measuring, Dipole Radiation, Acoustic Arrays

19 ABSTRACT (Continue on reverse if necessary and identify by block number)

A computer-controlled system for automated, remote measurement of phase and amplitude shaded doublet, triplet, and quadruplet acoustic arrays beam patters was developed and tested. Experimental data were collected with an anechoic chamber to minimize backscatter and other interference effects.

Preliminary impedance, reactance and resistance plots were made on several speakers to ensure that a matched set with similar characteristics was utilized for the arrays. Once the arrays were established, a computer program was developed for an HP-86 computer which allowed it to rotate the arrays, sample and collect data, and plot the results.

Various combinations of amplitude and phase shading were applied to the dipole, tripole, linear quadrupole and quadratic quadrupole array. The results were then

20 DISTRIBUTION/AVAILABILITY OF ABSTRACT	21 ABSTRACT SECURITY CLASSIFICATION	
XX UNCLASSIFIED/UNLIMITED ☐ SAME AS RPT ☐ DTIC USERS	Unclassified	
22a NAME OF RESPONSIBLE INDIVIDUAL: Alan B. Coppens	22b TELEPHONE (Include Area Code): 408-646-2941	22c OFFICE SYMBOL: 61Cz

DD FORM 1473, 84 MAR — 83 APR edition may be used until exhausted; All other editions are obsolete

SECURITY CLASSIFICATION OF THIS PAGE

19. ABSTRACT (continued)
compared to computer generated beam patterns which agreed to ± 2dB. This uncertainty was mainly generated by the slight deviations in the positioning of elements.

Approved for public release; distribution is unlimited.

Development, Validation and Use of a Computer-Controlled System for the Investigation of Phase and Amplitude Shaded Acoustic Arrays

by

John D. Butler
Lieutenant Commander, United States Navy
B.S., University of Texas at Austin, 1974

Submitted in partial fulfillment of the requirements
for the degree of

MASTER OF SCIENCE IN ENGINEERING ACOUSTICS

from the

NAVAL POSTGRADUATE SCHOOL
December 1986

ABSTRACT

A computer-controlled system for automated, remote measurement of phase and amplitude shaded doublet, triplet, and quadruplet acoustic arrays beam patterns was developed and tested. Experimental data were collected with an anechoic chamber to minimize backscatter and other interference effects.

Preliminary impedance, reactance and resistance plots were made on several speakers to ensure that a matched set with similar characteristics was utilized for the arrays. Once the arrays were established, a computer program was developed for an HP-86 computer which allowed it to rotate the arrays, sample and collect data, and plot the results.

Various combinations of amplitude and phase shading were applied to the dipole, tripole, linear quadrupole and quadratic quadrupole array. The results were then compared to computer generated beam patterns which agreed to ± 2dB. This uncertainty was mainly generated by the slight deviations in the positioning of elements.

TABLE OF CONTENTS

I. INTRODUCTION 11

A. PURPOSE OF THE STUDY 11

B. BACKGROUND 11

C. REPORT OVERVIEW 13

II. THEORY 15

A. DIPOLE RADIATION - ACOUSTIC APPROACH 15

B. LINEAR SYSTEMS 19

C. GENERAL QUADRUPOLE 23

III. EXPERIMENTAL PROCEDURE AND DEVELOPMENT 26

A. BEAM PATTERN MEASURING OVERVIEW 26

B. BEAM PATTERN PROGRAM 28

C. EXPERIMENTAL APPARATUS DEVELOPMENT 31

IV. DATA ANALYSIS AND VERIFICATION 36

A. THEORETICAL BEAM PATTERN PREDICTION 36

B. EXPERIMENTAL DATA-SINGLE ELEMENT DIRECTIONALITY 39

C. EXPERIMENTAL AND THEORETICAL DATA-VARIOUS ARRAY CONFIGURATIONS 42

D. EFFECTS OF ARRAY TILT, THETA 53

E. ERRORS 58

F. VALIDATION OF RESULTS 59

V. CONCLUSIONS AND RECOMMENDATIONS 65

APPENDIX A: EQUIPMENT DESCRIPTION 67

APPENDIX B: COMPUTER PROGRAM LISTING 74

APPENDIX C: EXPERIMENTAL AND THEORETICAL PLOTS 80

LIST OF REFERENCES 89

BIBLIOGRAPHY 90

INITIAL DISTRIBUTION LIST 92

LIST OF TABLES

I. ID-30 Driver Unit Resonant Frequencies 33

II. Array Configurations 64

III. Typical Program Data Collection Output 78

IV. Typical Calculated Beam Pattern Output 79

LIST OF FIGURES

2.1 Geometry used in Deriving the Radiation Characteristics of an Acoustic Dipole 16

2.2 Cartesian and Polar Representation of Pressure Amplitude Distribution of Dipole Radiation 17

2.3 Directional Diagrams of Various Combinations of Bidirectional and Nondirectional Microphones..... 18

2.4 Dipole Geometry 19

2.5 Axial Quadrupole Geometry 21

2.6 Tesseral Quadrupole Geometry 22

2.7 Quadrupole Geometry 24

3.1 System Diagram 27

3.2 Typical ID-30 Resistance Plot 32

3.3 Array Configurations 34

4.1 Three Dimensional Dipole Representation 37

4.2 Sectored Three Dimensional Plot (4 elements) 38

4.3 Polar Plot of a Four Element Array 40

4.4 ID-30 Acoustic Driver Directionality 41

4.5 Laboratory Dipole Plot 43

4.6 Theoretical Dipole Plot 44

4.7 Laboratory Three Element Isosceles Plot 46

4.8 Theoretical Three Element Isosceles Plot 47

4.9 Beam Pattern for 30° Tilt in Theta 49

4.10 Beam Pattern for 60° Tilt in Theta 50

4.11 Beam Pattern for 90° Tilt in Theta 51

4.12 Array Configuration for Tilt Theta 52

4.13 Laboratory Planar Quadruplet Plot 54

4.14 Theoretical Planar Quadruplet Plot 55

4.15 Laboratory Axial Quadrupole 56

4.16 Z-axis Offset Effects 58

4.17 kD_i = 9.5 for Error Computation 60

4.18 kDi = 10.0 for Error Computation 61

4.19 kD_i = 10.5 for Error Computation 62

A.1 Circuit Diagram for Modified Motor-Power/ Direction Controller 70

A.2 Data Acquisition Connection to Motor-Power Controller 73

C.1 Laboratory Three Element Isosceles Plot 80

C.2 Theoretical Three Element Isosceles Plot 81

C.3 Laboratory Planar Quadrupole Plot 82

C.4 Theoretical Planar Ouadrupole Plot 83

C.5 Beam Pattern for 0° Tilt in Theta (Tripole Isosceles) 84

C.6 Beam Pattern for 30° Tilt in Theta (Tripole Isosceles) 85

C.7 Beam Pattern for 90° Tilt in Theta (Tripole Isosceles) 86

C.8 Beam Pattern for 60° Tilt in Theta (Planar Quadrupole) 87

C.9 Beam Pattern for 90° Tilt in Theta (Planar Quadrupole) 88

ACKNOWLEDGEMENTS

I would like to express my gratitude and heartfelt thanks to those who, through their assistance and encouragement, made this work possible. First, to Dr. Alan Coppens and LCDR Greg Netzorg, my thesis advisor and co-advisor, who were always available for guidance and direction. I would also like to thank my wife, Eileen, who was ever present to provide encouragement during the past two and one half years.

I would like to dedicate this work to the three most important people in my life: my wife, Eileen, and my sons, Dale and Jack. It was their support and love which made this endeavor possible.

I. INTRODUCTION

A. PURPOSE OF STUDY

The purpose of this investigation was to develop and verify a computer-controlled experimental system to measure and plot the pressure fields of various acoustic arrays in an anechoic environment. This was to be done using various combinations of phase shading and amplitude shading of doublets, triplets, and quadruplets. Experimentation was conducted under computer control to maximize the amount of data available and to ensure the highest degree of accuracy. Additionally, a comparison was conducted with the theoretical predictions obtained by Park [Ref. 1].

B. BACKGROUND

The use of dipoles and quadrupoles for beam forming and direction finding, both in air and in water, has been a subject of intense investigation since the 1940's. The basic radio direction finding apparatus of the 1940's was nothing more than a set of orthogonal dipoles which consisted of two crossed loops. The relative signal amplitude from the two dipoles was used to determine the direction of arrival of a signal. The angle is equal to Arctan (y/x) where x was the amplitude of one dipole and y, the amplitude of the other dipole. This presented a 180°

bearing ambiguity which was resolved by comparing the phase of the x and y dipole signals with the phase of a co-located omni-directional antenna. [Ref. 2]

In the 1950's, extensive studies were conducted using planar arrays with multiple acoustic and electromagnetic dipole elements. These studies led to the formulation of planar arrays employed in radar systems of the 1960's. Further research resulted in the ability to steer beam patterns by use of multiple elements, phase shading, and amplitude shading.

In 1976, work was done by Hughes and Thompson to investigate acoustic communications, particularly in underwater acoustics for cases where the position of the source or the receiver is fixed. They investigated the tilted directional response patterns below the horizontal plane due to amplitude weighting and a single 90° phase shift. Here, a method of achieving a tilted pattern from a symmetrically shaped array without using numerous phase shifts or time delays was discussed. [Ref. 3] Moses and Smith also examined beamforming this time with a cylindrical array using real (rather than complex) shading coefficients [Ref. 4].

In 1985, Flanagan examined the use of computer-steered microphone arrays which were two-dimensional planar arrays of 9 x 7 elements. Here an array was designed and computer steered to discriminate against sound arrivals from all but the desired directions. [Ref. 5]

One example of the Navy's current use of dipole technology is in sonobuoys. The SSQ-53 DIFAR Sonobuoy possesses both an omnidirectional and bi-directional hydrophone capability. The SSQ-77A VLAD Sonobuoy possesses an upper and lower array strung in a single line array. Beamforming is accomplished by the use of both phase shading and amplitude shading.

These advancements in the study of arrays ranging from a single dipole to large scale planar arrays, coupled with computer control, form the basis for this further study of shaded arrays. There is currently a related research effort ongoing in the study of computer controlled arrays and beam patterns being conducted by the Environmental Physics group at the Naval Postgraduate School.

C. REPORT OVERVIEW

In Chapter II, a basic introduction to theoretical pressure and directivity calculations of a dipole is developed. This is then used as a base to expand to the physical case and the electrical linear systems case. Finally, these results are applied to different forms of quadruplets and triplets to show theoretically, the expected results.

Chapter III contains a summary of the beam pattern measuring system, the computer program development, experimental procedure, and representative data and plots.

Additionally, it provides a description of the system which was assembled for measuring the pressure fields of the various arrays.

Chapter IV contains a summary of data analysis and verification. Additionally, representative plots are provided for amplification of arguments.

Chapter V contains concluding remarks and recommendations for further work.

Appendix A provides a brief description of each piece of equipment and summary of its capabilities as applied to this experimental investigation.

Appendix B lists the BASIC computer language program used for data acquisition and formulation in this study.

Appendix C contains specific plots, both experimental and theoretical, obtained as a result of this investigation and that of Park [Ref. 1]. These plots were obtained for beam patterns of various array configurations.

II. THEORY

The dipole has been extensively explored and is now utilized as a basic unit in the construction of a great many arrays and antennae. In this section we will elucidate the theory using two approaches 1) an acoustic approach in 2 dimensions and 2) a linear systems approach in three dimensions. These two approaches are related to each other and yield the same result after minor changes are made in the geometry of the problem. Both are presented because of direct Navy applications dealing deal with SONAR arrays.

Following the presentation of each of these, the equations for the triplet and quadruplet arrays utilized in this research effort will be shown.

A. DIPOLE RADIATION-ACOUSTIC APPROACH

Because it is usually desirable and useful to be able to determine the direction from which an acoustic signal originated, arrays were developed to provide this information; a simple example of this is the acoustic dipole. A simple dipole consists of two simple sources of equal strength but opposite phase, separated by a distance d Fig. (2.1).

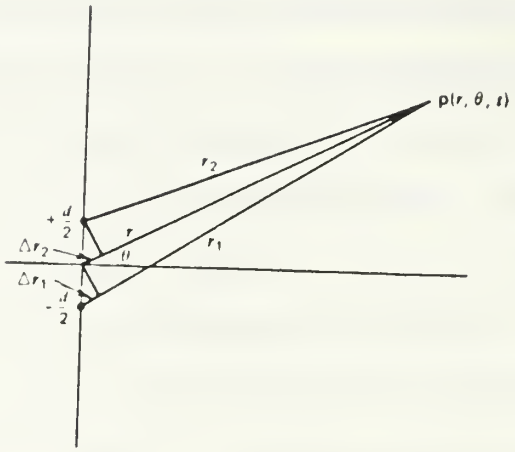

Figure 2.1 Geometry used in Deriving the Radiation Characteristics of an Acoustic Dipole.

The pressure, $p(r,\Theta,t)$, measured at the field point (r,Θ) due to source 1 and 2 respectively are

$$P_1 = [A/(r + \Delta r_1)] \exp[j(\omega t - k(r + \Delta r_1)] \quad (1)$$

$$P_2 = [-A/(r - \Delta r_2)] \exp[j(\omega t - k(r + \Delta r_2)] \quad (2)$$

where A is the pressure amplitude of an individual source measured at one meter from the source, r is the distance from the field point to the midpoint between the sources, $\omega = 2\pi f$ is the angular frequency and k is the wave number. The minus sign associated with P_2 accounts for the 180° phase difference. The total acoustic pressure is the sum of

P_1 and P_2,

$$P(r,\theta,t)=(A/r)\{\{[\exp(-jk\Delta r_1)]\,[1+(\Delta r_1/r)]\}-\{[\exp(-jk\Delta r_2)]/[1+(\Delta r_2/r)]\}\}\exp(j(\omega t-kr)) \quad (3)$$

Considering only field measurements where the separation d is small compared to the distance r, we can use the far field approximations, $\Delta r_{1,2} = (d/2)\sin\theta$ and $\Delta r_{1,2}/r << 1$. This yields the acoustic dipole radiation pressure field,

$$P(r,\theta,t) = -j\,(2A/r)\sin\{(kd/2)\sin\theta)\}\exp j(\omega t - kr) \quad (4)$$

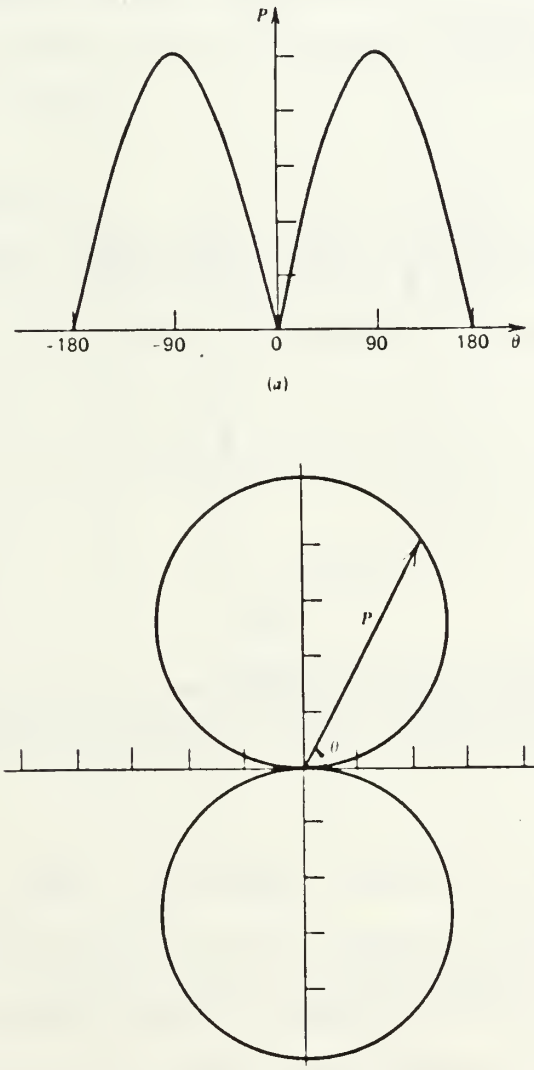

Figure 2.2 Cartesian and Polar Representation of Pressure Amplitude Distribution of Dipole Radiation. [Ref. 6]

As noted in Eq. (4) and seen in Fig. (2.2), plotting the far field for $d << \lambda$, pressure nulls exist when $(kd/2)\sin\Theta = \pi n$ where n is an integer. [Ref. 6]

The twin lobes and nulls of a dipole result in an 180° ambiguity when trying to localize a source. If the dipole is combined with an omnidirectional receiver, the ambiguity can be resolved. In Fig. (2.3), various combinations of dipole and omnidirectional receivers are combined to provide a cardioid response.

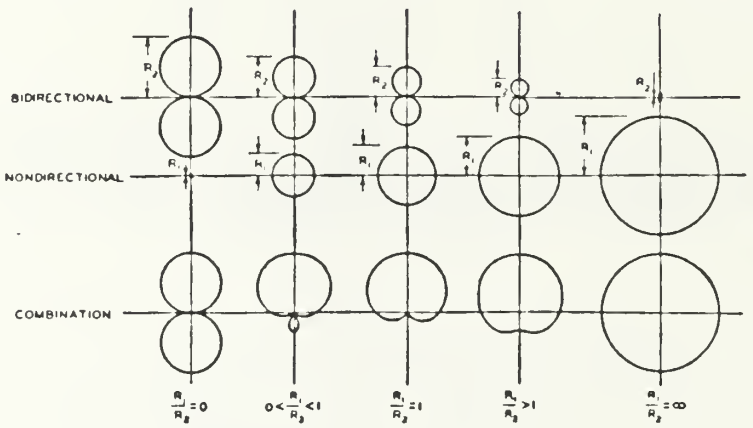

Figure 2.3 Directional Diagrams of Various Combinations of Bidirectional and Nondirectional Microphones. [Ref. 7]

Here R_1 is the voltage output of the omnidirectional receiver and R_2 the voltage output of the directional dipole receiver. It is not important for the two sources to be of the same sensitivity, but the ratio R_1/R_2 must be unity for true cardioid response. The phase shift between these two

receivers, which yields directionality, is achieved through a difference in the phase characteristics of the omni which is differentiated (high pass filtered) to compensate for the linear frequency dependence of the dipole sensitivity. [Ref. 7].

This design is presently used in SSQ-77A VLAD Sonobuoys where a cardioid is formed pointing in the downward direction. This maintains the null in the upward direction in order to alleviate high frequency interference from wind and sea surface noise.

B. LINEAR SYSTEMS

Consider the geometry for a dipole as shown in Fig. (2.4):

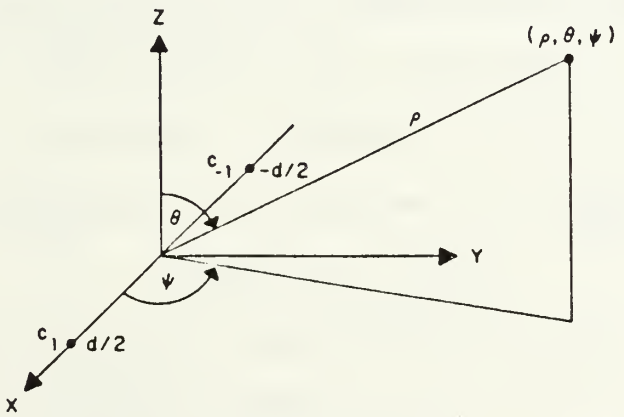

Figure 2.4 Dipole Geometry [Ref. 8]

In this representation as developed in Ref. (7), C_1 and C_{-1} are complex weighted point sources which are free to rotate in the x-y plane and d is the distance between elements. The complex weighted response factor c_i of the ith point source is

$$c_i = a_i \exp(j\varphi_i) \tag{5}$$

where ai is the amplitude and Ψ_i is the phase angle. For a dipole, the complex weighted response factors are $c_1 = a_1$ and $c_{-1} = -a_1$.

For a wave originating from a distant source and propagating to the receiver, it is observed that there is an essentially constant pressure magnitude over the dipole aperture. Because the phase varies with position along the wave front in a traveling wave, the response of the dipole is given as a function of frequency and direction cosine u where $u = \sin\Theta\cos\Psi$. The response is

$$D(f,u) = c_1 \exp(j\pi du/\lambda) + c_2 \exp(-j\pi du/\lambda) \tag{6}$$

This equation is simplified for the dipole to:

$$D(f,u) = 2ja_1 \sin(\pi du/\lambda) \tag{7}$$

Since u is a direction cosine, it is only valid over the interval $-1<u<1$. As a result, $0 \le \theta \le \pi$ and $0 \le \psi \le 2\pi$. u = o implies a broadside or on-axis geometry and u = 1 implies an end-fire geometry. A plot of D(f,u) as a function of u can be used to approximate the response of a dipole. [Ref. 8]

An example of this two element response of two point sources with a separation d equal to one half the wavelength of the traveling wave results in a real response for values of u from $(-\lambda/2d)$ to $(+\lambda/2d)$. If the sources are assigned dipole weightings, substitution of the functions Θ and Ψ for direction cosine u result in the unnormalized, far field beam pattern

$$D(f,\theta,\psi) = j2a_1 \sin[(\pi d/\lambda) \sin\theta \cos\psi] \qquad (8)$$

This linear systems theory can be easily applied to the axial quadrupole and Tesseral quadrupole. The axial quadrupole is an array of three complex weighted point sources where $c_1 = a_1 = c_{-1} = a_{-1} = 1$ and $c_o = a_o = -2$ as in Fig. (2.5).

Here C_o can also be thought of as 2 sources with each having an amplitude weight equal to -1.

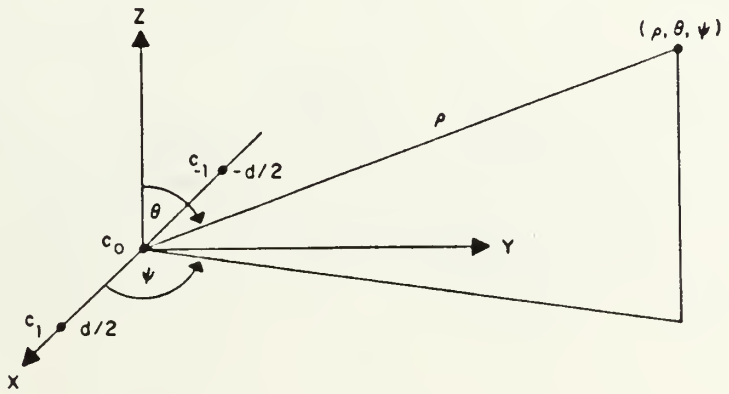

Figure 2.5 Axial Quadrupole Geometry [Ref. 8]

With the 1,-2,1 amplitude weighting, the far-field, unnormalized directivity function is defined as:

$$D(f,f_x) = [\exp(-j2\pi f_x d/2)] - 2 + [\exp(j2\pi f_x d/2)] \quad (9)$$

where $f_x = u/\lambda = \sin\theta\cos\psi/\lambda$. This reduces to:

$$D(f,\theta,\psi) = 2\,[\cos\{(\pi d/\lambda)\sin\theta\cos\psi\} - 1] \quad (10)$$

In the case of a Tesseral quadrupole Fig. (2.6), a planar array of four amplitude-weighted point sources, the unnormalized directivity function is:

$$D(f,f_x,f_y) = 2Q\cos[\pi d(f_x + f_y)] - 2Q\cos[\pi d(f_x - f_y)] \quad (11)$$

where $f_x = u/\lambda = \sin\theta\cos\psi/\lambda$, $f_y = v/\lambda = \sin\theta\sin\psi/\lambda$ and the direction cosine $v = \sin\Theta\sin\Psi$. This yields

$$D(f,\theta,\psi) = -4Q\sin[(\pi d/\lambda)\sin\theta\cos\psi]\sin[(\pi d/\lambda)\sin\theta\sin\psi] \quad (12)$$

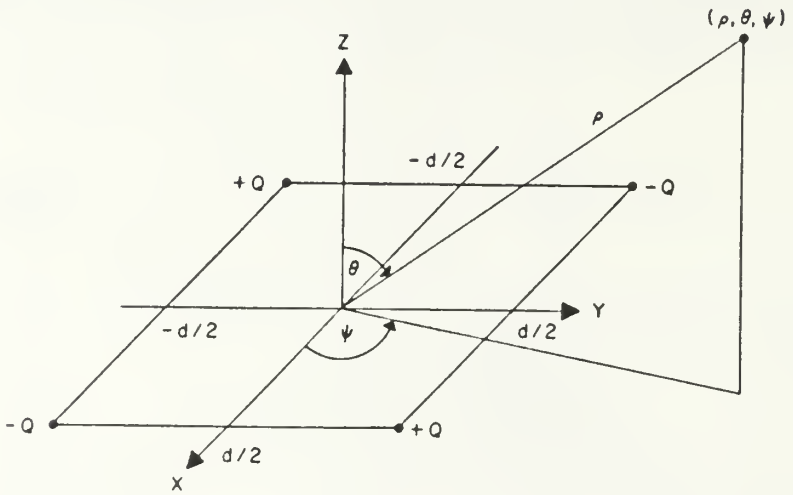

Figure 2.6 Tesseral Quadrupole Geometry

which is the far field, unnormalized directivity function for this quadrupole as a function of Θ and Ψ. [Ref. 8] The above development is particularly important because this type array was investigated in the course of this work.

C. GENERAL QUADRUPOLE

Park, in his thesis (Ref. 1), developed an equation for calculation of a four element array Fig. (2.7). The equation was developed by adding complex pressures from four sources to yield

$$P = \frac{1}{R} e^{j(\omega t - kR - kD_1 \sin\theta\sin\Phi)} + \frac{A}{R} e^{j(\omega t - kR + kD_2 \sin\theta\sin\Phi - \varphi_2)} \quad (13)$$
$$+ \frac{B}{R} e^{j(\omega t - kR + kD_3 \sin\theta\cos\Phi - \varphi_3)}$$
$$+ \frac{C}{R} e^{j(\omega t - kR - kD_4 \sin\theta\cos\Phi - \varphi_4)}.$$

where $[(1+A+B+C)/R]\exp[j(\omega t - kR)]$ is the maximum possible pressure amplitude and the distances D_1, D_2, D_3, D_4 and measured from the origins to the particular element. The directivity is:

$$H(\theta,\Phi) = \frac{1}{(1+A+B+C)}\{[\cos(kD_1\sin\theta\sin\Phi) + A\cos(kD_2\sin\theta\sin\Phi - \varphi_2) \quad (14)$$
$$+ B\cos(kD_3\sin\theta\cos\Phi - \varphi_3) + C\cos(kD_4\sin\theta\cos\Phi + \varphi_4)]^2$$
$$+ [\sin(kD_1\sin\theta\sin\Phi) - A\sin(kD_2\sin\theta\sin\Phi - \varphi_2)$$
$$- B\sin(kD_3\sin\theta\cos\Phi - \varphi_3) + C\sin(kD_4\sin\theta\cos\Phi + \varphi_4)]^2\}^{1/2}$$

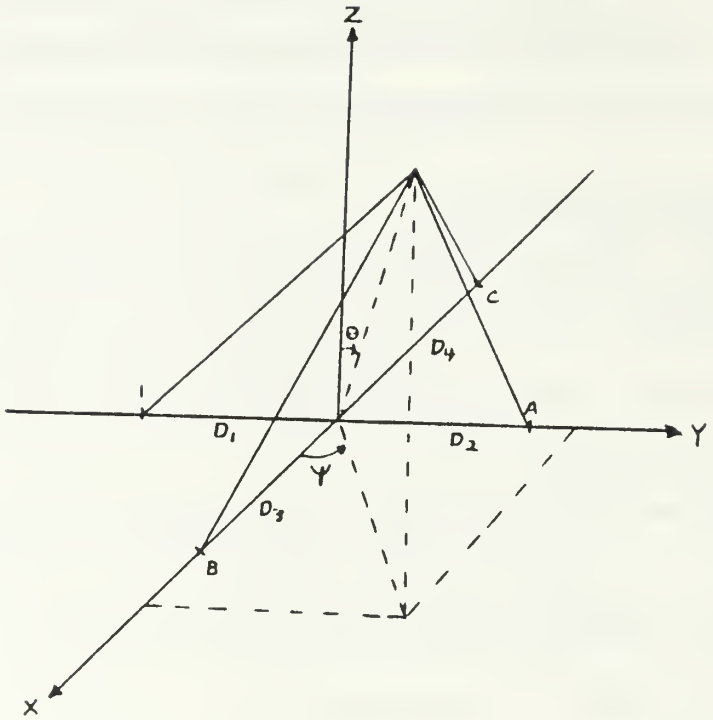

Figure 2.7 Quadrupole Geometry

If $D_1 = D_2 = D_3 = D_4$ then comparison of Figs. (2.7) and (2.6) shows that the configuration is simply the Tesseral quadrupole of Fig. (2.6) where Ψ has been shifted 45°.

Additionally, the axial quadrupole of Fig. (2.5) is obtained using Park's program by placing source B at an infinitesimally small distance from the array center (i.e., D3 = 0.00001 meters for any λ) with amplitude weighting equal to twice sources 1 and A and source C amplitude weighted to zero, which removes its contribution

from the array. This axial quadrupole can also be obtained by placing sources B and C at the array center and amplitude weighting equally.

These equations were utilized to provide verification data for the laboratory experiments. The three element array data were verified by amplitude weighting element C of Eq. (14) to zero. Dipole data were verified by amplitude weighting elements B and C of Eq. (14) to zero.

III. EXPERIMENTAL PROCEDURE AND DEVELOPMENT

A. BEAM PATTERN MEASURING SYSTEM OVERVIEW

The beam pattern measuring system is an instrumentation package which was designed to power and rotate an acoustic array and then receive the signal, compute the pressure distribution of the array and display this data in both a tabulated format and plot of sound pressure level in decibels versus degrees of rotation. All data were taken in an anechoic chamber to minimize surface interference.

The system used for measuring beam patterns of different arrays is divided into two major groups. These are the signal generation and input section and the automated advancement, data collection and display section. An overview of these is now presented along with a block diagram of the system, Fig. (3.1). A detailed description of each piece of equipment is contained in Appendix A.

The Hewlett-Packard (HP) Function Generator Model 3314A was utilized for all signal generation. The signal passed through an individual HP-467A Power Amplifier to each of the University Sound Model ID-30 acoustic driver units. Setting the output levels of the driver units was accomplished utilizing the variable gain control on the power amplifiers. This constituted the signal generation and input section.

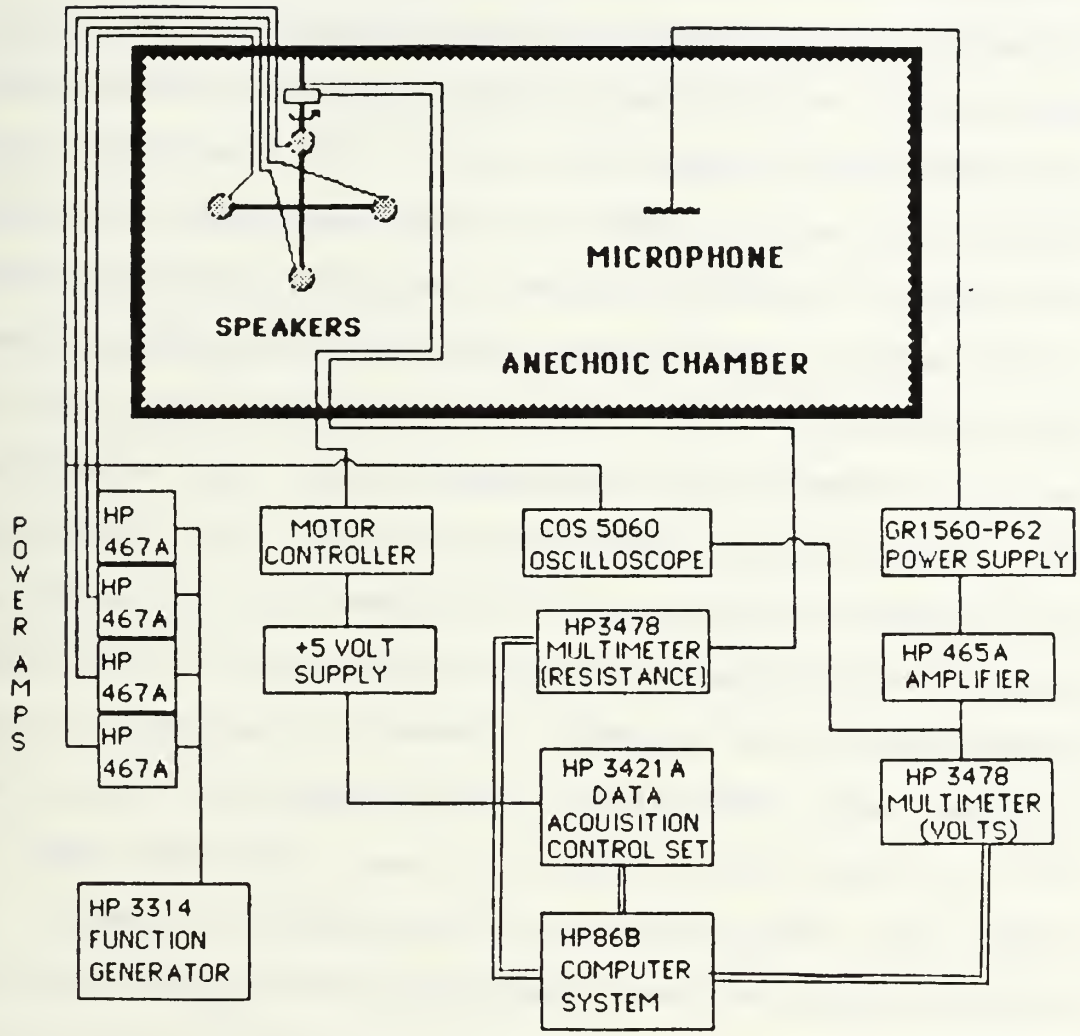

Figure 3.1 System Diagram

The receiving and processing section was controlled by the HP-86B computer. It directly controlled the array rotation and the reading of all measurements of peripheral instruments via the Hewlett-Packard Interface Bus (HPIB). The computer sent clockwise stepping commands to the motor-power/direction controller via the HP-3421A Data Acquisition/Control (DAC) to rotate the array in stepped increments of about one degree. Following each advancement of the array, the computer read both the resistance output of the array rotation measurement potentiometer and the voltage output of the General Radio Model 1962 Microphone. The array rotation potentiometer was a Ø to 1Ø Kohm potentiometer mounted on top of the rotation motor and measured the angle of rotation of the array (Ø to 1Ø Kohms corresponded to $Ø^{o}$ to $36Ø^{o}$). These resistance and voltage readings were then stored in the computer for use in the data analysis and plotting routines. Once the data was taken for $36Ø^{o}$ of rotation, it was used to compute the rotation angle and its corresponding decibel (dB) level for each datum. These values were then output to the computer monitor and plotted in the form of a polar plot of dB versus degrees of rotation.

B. BEAM PATTERN PROGRAM

The Beam Pattern program listed in Appendix B, consists of a series of sub routines. The program starts by

providing addresses for the two multimeters and the data acquisition/control unit. Next the initialization subroutine resets and initializes these three instruments.

Once the equipment is ready to operate, the incrementing subroutine is called. This is an iterative and interactive routine used to rotate the array and measure the voltage of the sensed pressure field and the corresponding resistance reading which is proportional to the angular position of the array. Up to 360 data points can be collected per data run. After the initial datum is read, the array rotator motor is energized for 0.5 milliseconds to increment the array azimuth. The array is then allowed to coast down for 4 seconds prior to reading the voltage and resistance. This selection of rotate and coast down times is discussed later in the chapter. Once the resistance and voltage readings are taken, they are stored in an array for later transfer to a data disk and for use in the plot subroutine.

Finally the plot subroutine calculates the relative decibel level of the beam pattern based on the measured voltages. It then takes the resistance reading and converts it to the angle of rotation. The calculated decibel levels are then normalized to zero decibels based on the highest received voltage reading. Finally, the data points are plotted on a polar plot of relative sound pressure level in decibel versus angle of rotation.

All raw data is stored on a data disk after a complete data run. Each data run is stored by run number, as shown in Table II. It can be retrieved and printed at the printer as received voltage and resistance for each datum point or printed and plotted as decibel versus angle of rotation.

The physical weight of an array was a major variable in this program with regard to the selection of the number of data points needed. Arrays weighing less than 4 pounds required 360 data points for a full 360° of rotation. The number of data points required for larger arrays was decreased as array weight increased. For the four element array, weight was substantial enough (19 pounds) to require only 317 data points for a full 360° rotation. This was caused by the fact that the heavier arrays would coast-down for a larger distance after the 0.5 millisecond motor-on period.

Another contributor to variation in the required number of data points was array balance. When utilizing a three element array, the array was sufficiently out of balance to require a greater number of data points for full rotation. This was attributed to minor binding of the rotator shaft as the array coasted down.

Selection of motor run time and coast-down time was based on experimental investigation. A 0.5 millisecond motor on time provided 1° rotation regardless of coast-down

time with a light weight array. The 4 second coast-down was selected because smaller periods did not allow the array to stop and the resistance multimeter to stabilize prior to it being read. Motion at the variable potentiometer when the resistance values were read yielded erratic reading on the multimeter due to electromagnetic interference generated by the motor.

C. EXPERIMENTAL APPARATUS DEVELOPMENT

The experimental apparatus was designed to optimize a thorough search of two, three and four element arrays and to establish their respective beam patterns. Previously, several experimental investigations have been conducted utilizing a two microphone array with a single source. It was, therefore, decided that reciprocity would be invoked and the array would consist of multiple ID-30 driver units (Appendix A) with a single microphone utilized for sensing the pressure field.

Six ID-30 driver units were checked individually in the anechoic chamber for their beam pattern impedence, resistance and reactance characteristics. This data was utilized to select the best matched set of four driver units. All drivers were examined between 5 Hz and 3000 Hz in an effort to locate and identify the resonances in the individual speakers. Fig. (3.2) shows a representative resistance curve for these drivers between the above

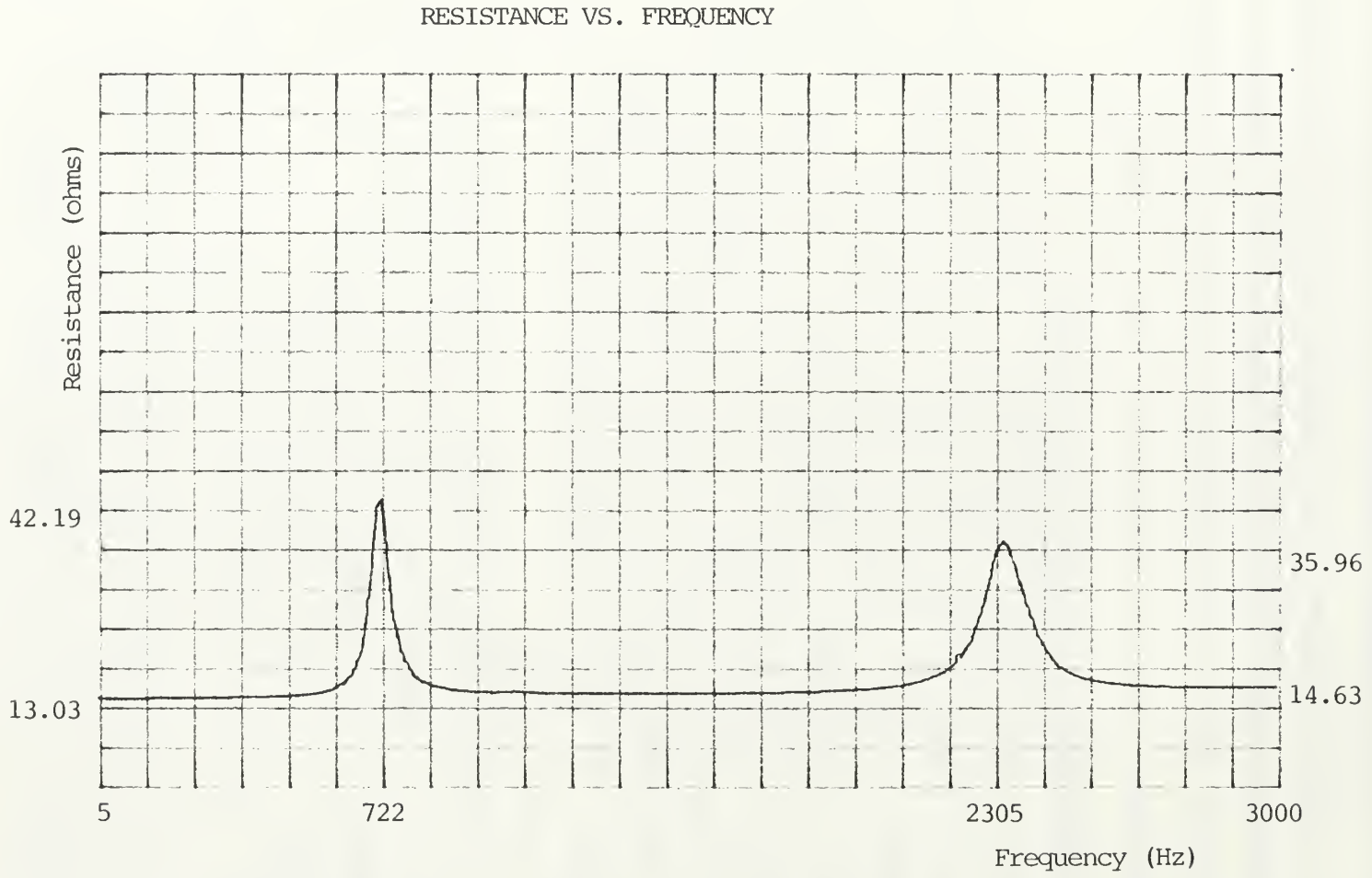

Figure 3.2 Typical ID-30 Resistance Plot

frequencies. It was desired to conduct all analysis at frequencies in relatively flat areas away from resonances. This was done to assure phase stability since reactance is not varying. The speakers utilized in this investigation had resonances as per Table I.

TABLE I

ID-30 DRIVER UNIT RESONANT FREQUENCIES

Speaker Number	First Resonance (Hz)	Second Resonance (Hz)
1	689	2290
2	660	2225
3	780	2150
4	798	2129
5	740	2253
6	778	2125

Matched set number 1 consisted of speakers 1 and 2 and set number 2 of speakers 3 and 4. All array beam patterns were run at 300 Hz and 960 Hz which fell in the flat areas of the impedance curves.

The array existed in two individual configurations, a linear and a crossed axis system with variable tilt (Fig. (3.3)). The linear system was used for investigation of doublets, some triplets and quadruplets (in the form of an axial quadrupole). The crossed axis array proved to be extremely versatile and useful, providing four arms, each 70 centimeters in length, for holding the drivers.

Additionally, it provided a means to vary the angle Θ a full 90^{o}. Each driver was equipped with a harness assembly which mounted to the array rod in such a manner that the driver face was located 2.5 centimeters off the axis. This did not prove to be a matter of concern since all pressure measurements were made in the far field.

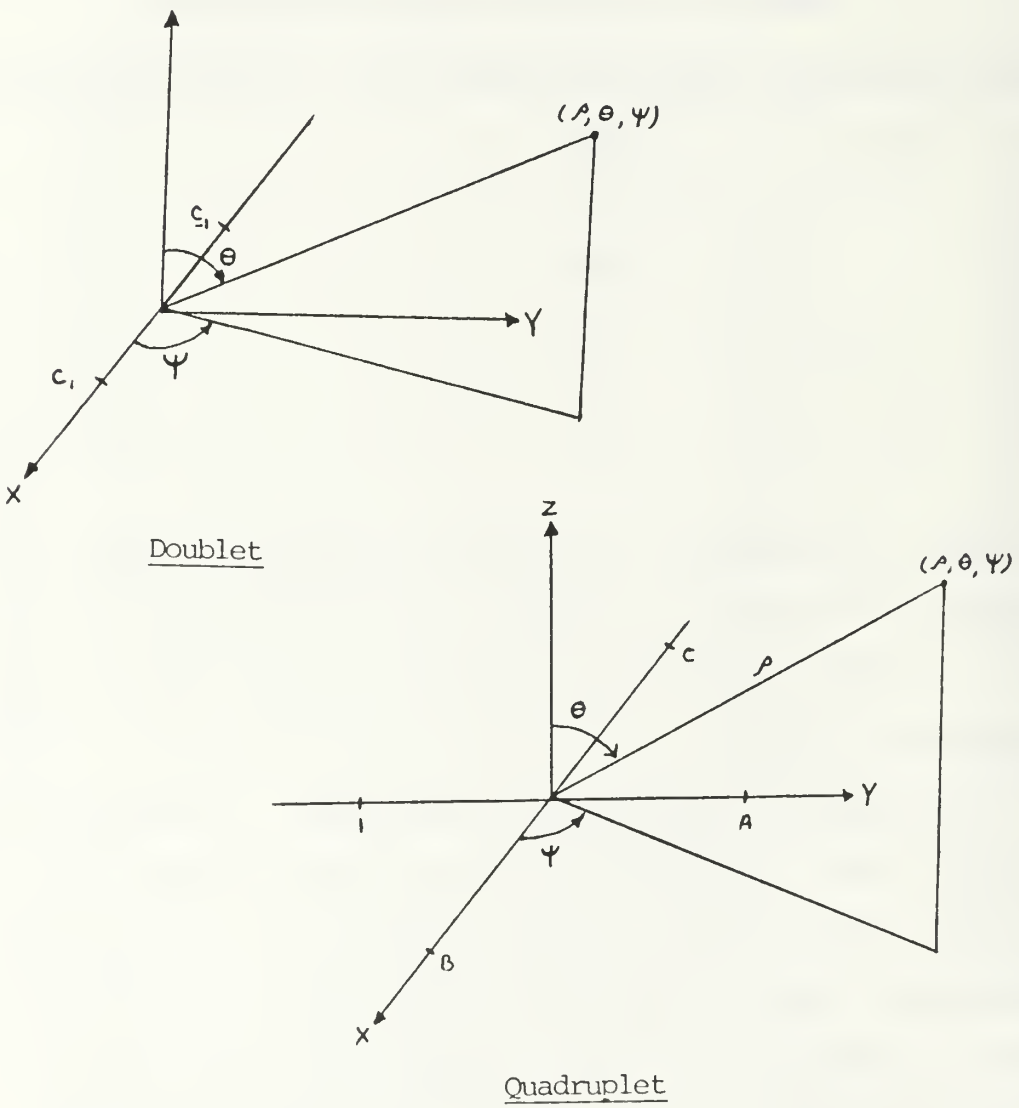

Figure 3.3 Array Configurations

A scattering and shading problem of small magnitude was encountered because of the large center piece on the crossed axis array. This scattering problem was largely resolved by wrapping the center piece with fiberglass.

The General Radio Model 1962 microphone was located 3.2 meters from the center of the array placing it in the far field. It was mounted at the same height in the anechoic chamber as the array center. Changes in tilt angle theta were accomplished by tilting the array.

The outputs of the ID-30 driver units were balanced prior to each data run. It was done by aligning the array in the vertical plane with the drivers facing the microphone. Then the output of each driver was adjusted utilizing the variable gain control on the power amplifier. This allowed all the drivers to be driven within a received voltage of 0.002 VAC of each other out of a typical level of 1 Volt.

Output signals from the HP-467A Power Amplifiers were monitored on an oscilloscope as was the received signal from the microphone. Because the signals were clean and without any substantial noise, filters were not utilized in the microphone circuit.

IV. DATA ANALYSIS AND VERIFICATION

After establishing the ability to accurately rotate an acoustic array while collecting and displaying sensed pressure levels under computer control, it was necessary to ensure the data were accurate. This could be done by taking a set of parameters and obtaining both theoretical and experimental beam patterns for them. Verification was conducted utilizing the results of a FORTRAN program developed by Park (Ref. 1) which yields a variety of useful plots with the help of DISSPLA.

A. THEORETICAL BEAM PATTERN PREDICTION

With the program developed by Park, quick beam pattern plots could be made to compare with experimental patterns. As an example, Fig. (4.1) depicts a three dimensional representation of a dipole. Clearly, this particular is not of much use.

The three dimensional plot was sectored for greater utility. Fig. (4.2) shows a sector representation for a four element array with $kD_1 = kD_2 = 3.52$ and $kD_3 = kD_4 = 0$. Note that the kD_i utilized in the remainder of the thesis related directly to the spacing from the center of the array to the element as related to Fig. (2.7). Refer to Fig. (2.7). The Z-axis of the plot is beam pattern (dB), the Y-

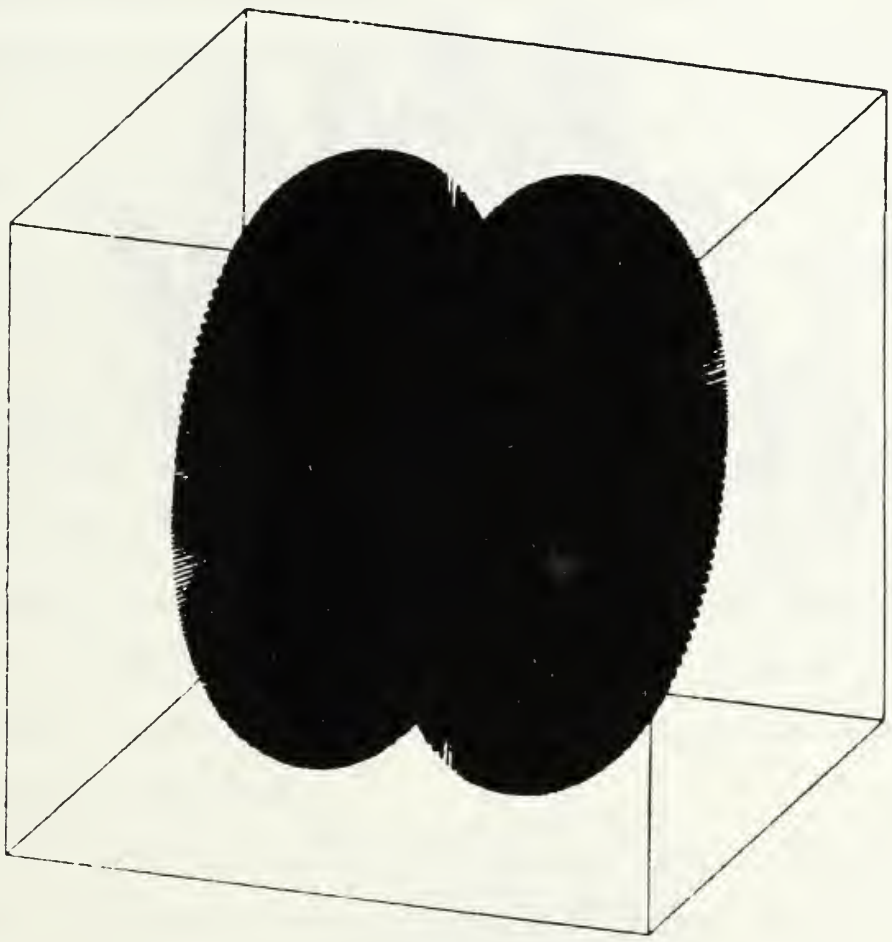

Figure 4.1 Three Dimensional Dipole Representation

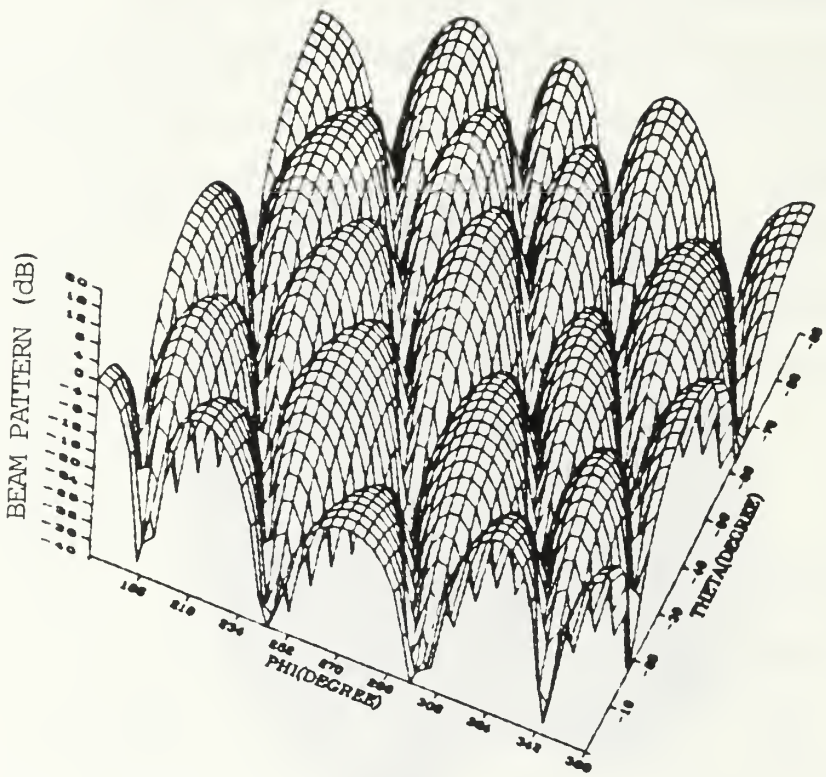

$kD_1=kD_2=kD_3=kD_4=$ 10.55

D1= 0.6 D2= 0.6
D3= 0.6 D4= 0.6
VIEW ANGLE=+20,+60
P2= 0 P3= 0 P4= 0
A=1. B=1. C=1.

Figure 4.2 Sectored Three Dimensional Plot (4 Element)

axis psi (degrees), and the X-axis theta (degrees). Directivity is scaled from 20 to -40 dB (with 0 dB being the highest achievable value because of normalization), psi from 180° to 360°, and theta from 0° to -90°. This plot appears to be very busy but proves to be quite useful. It is easy to evaluate this sectioned representation by following the contour line of the directivity above the line theta equals 0° for psi from 180° to 360°. This provides the same dB levels at $180^{\circ} < \text{psi} < 360^{\circ}$ as the polar plot representation plotted in Fig. (4.3).

B. EXPERIMENTAL DATA-SINGLE ELEMENT DIRECTIONALITY

As stated in Chapter III, testing was conducted at 300 Hz and 960 Hz which were in the flat areas of the drivers' resistance curves, away from their resonance peaks. This was done to assure phase stability between drivers since the reactance is not varying (large phase shifts do not occur except near resonance).

Initial data runs were conducted with a single ID-30 acoustic driver to establish the directionality of each of the drivers. The drivers were rotated 360° at three separate tilt angles of the driver face, $\Theta = 0^{\circ}$, 45° and 90°. A representative graph of the directionality is contained in Fig. (4.4) which was made with the driver at a tilt angle of 0° and pointing at the microphone prior to rotation. The dotted line is the laboratory beam pattern. Note that there

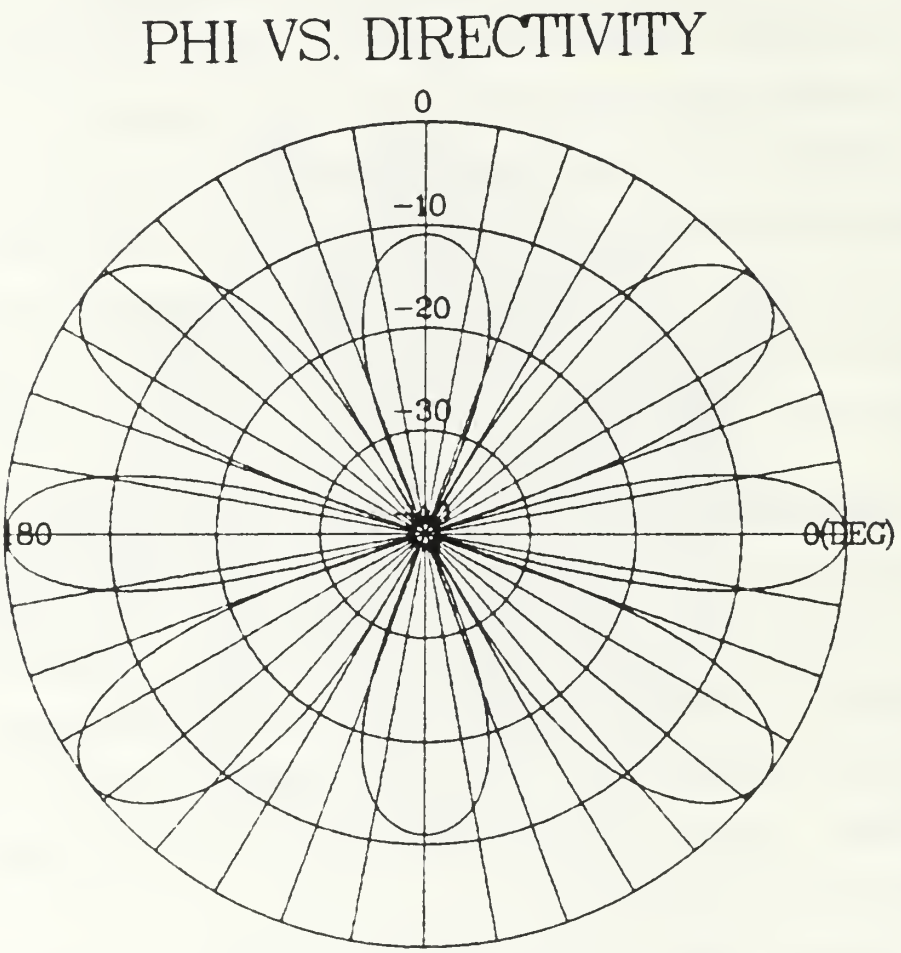

Figure 4.3 Polar Plot of a Four Element Array

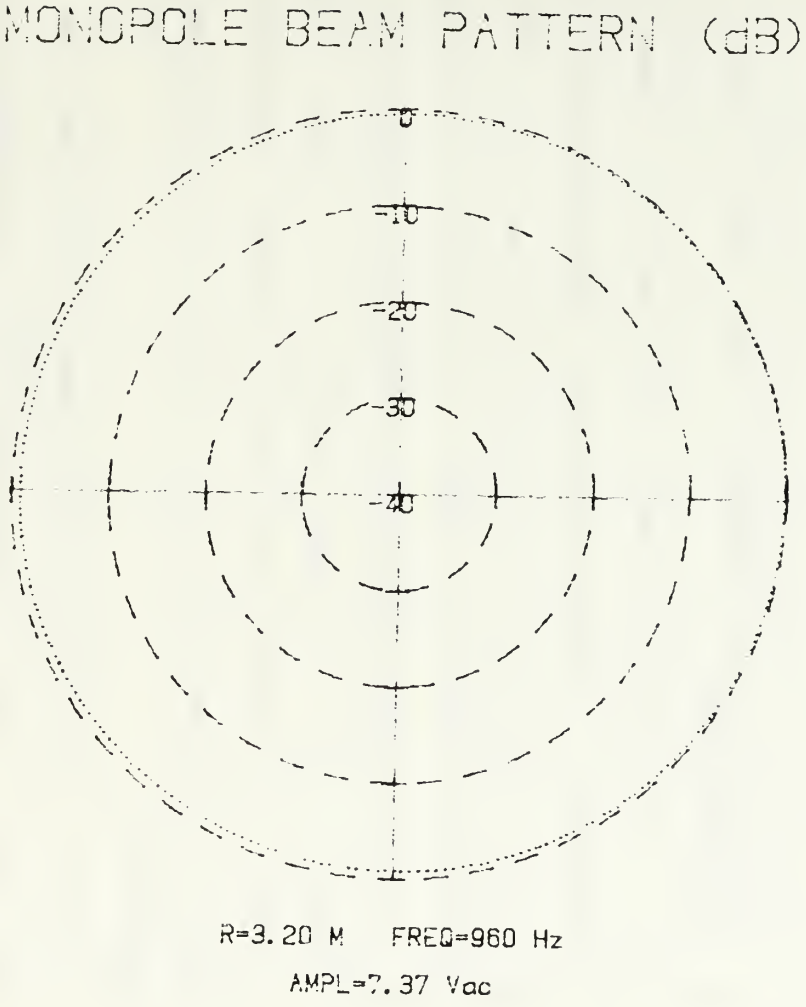

Figure 4.4 ID-30 Acoustic Driver Directionality

is a 1 to 2 dB drop below the 0 dB level as the driver points away from the receiver which shows the driver is not completely omnidirectional. It should also be noted that the program's normalization routine sets the highest received microphone voltage level to Ø dB and normalizes all other voltage levels in the beam pattern to this level. This was done to provide greater ease in plotting of beam patterns so as to produce a uniformity between plots.

C. EXPERIMENTAL AND THEORETICAL DATA - VARIOUS ARRAY CONFIGURATIONS

An investigation of two, three and four element arrays was conducted. For each of these configurations, several different combinations of spacing and amplitude and phase shading were looked at. Table 2 at the end of this chapter, is a list of these variations for which beam patterns were obtained. Note that phase shading was limited to either $\emptyset^{\circ}$ or 180°. In viewing the figures, the term "x-pole" is used loosely to represent the term "x-let" (i.e., quadrupole for quadruplet).

For the two element array, beam patterns were run in the laboratory for both in-phase and 180° out-of-phase doublets. An example of the out-of-phase doublet beam pattern obtained in the anechoic chamber is shown in Fig. (4.5). (Note that in this figure kd is the quantity $2kD$, when $D_1 = D_2$.) Its theoretical verification, obtained from Park's program is shown in Fig. (4.6). A contributing factor to their

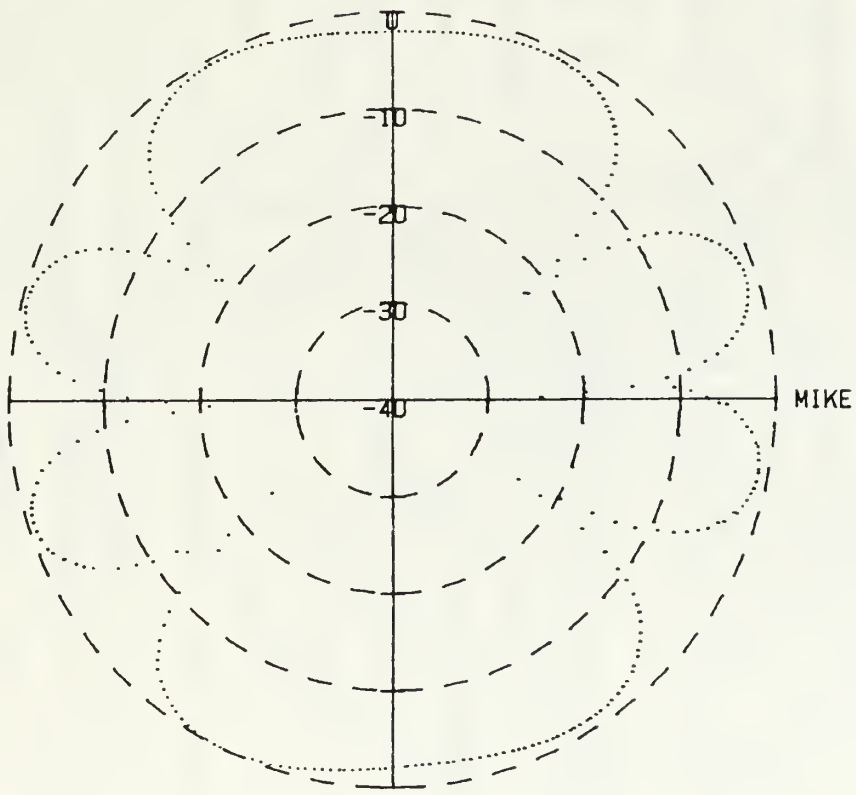

Figure 4.5 Laboratory Dipole Plot

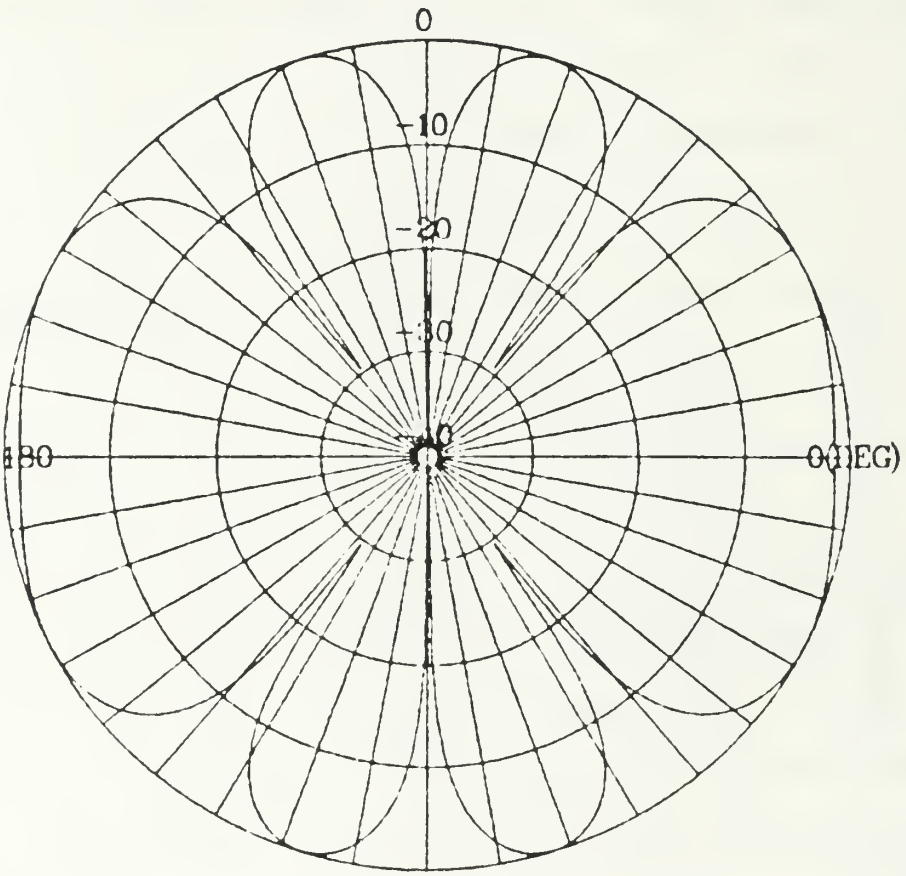

Figure 4.6 Theoretical Dipole Plot

small differences, is the slight directionality associated with the acoustic driver. The slight offset of the laboratory plot nulls is caused by the array not being exactly aligned to broadside at Ø Kohm on the potentiometer. The 90° rotation between the two plots is caused when theta is fixed at 90° vice 0° for theoretical plots. Because of the narrowness of the nulls, laboratory data would require a sample exactly with the array broadside to achieve the null. Other than the difference in nulls, there is exceptionally good agreement between experimental and theoretical beam patterns.

In the investigation of three element arrays, the arrays were configured as equilateral triangles, isosceles triangles and as a linear array. For phase shading, three cases were looked at: all elements in phase, the center element 180 out- of-phase, and one end element placed 180 out-of-phase. These arrays were also subjected to various amplitude shading (the axial quadruplet composed of three elements with the center element amplitude shaded to twice the value of each of the end elements will be discussed in the quadruplet section). Experimental data for a three element isosceles triangle with all elements in phase and $kD_1 = kD_2 = 2kD_3 = 5.28$ are shown in Fig. (4.7) with its theoretical verification shown in Fig. (4.8). The deep theoretical nulls seen on Fig. (4.8) are not present in the laboratory data. This can be attributed to a small variance

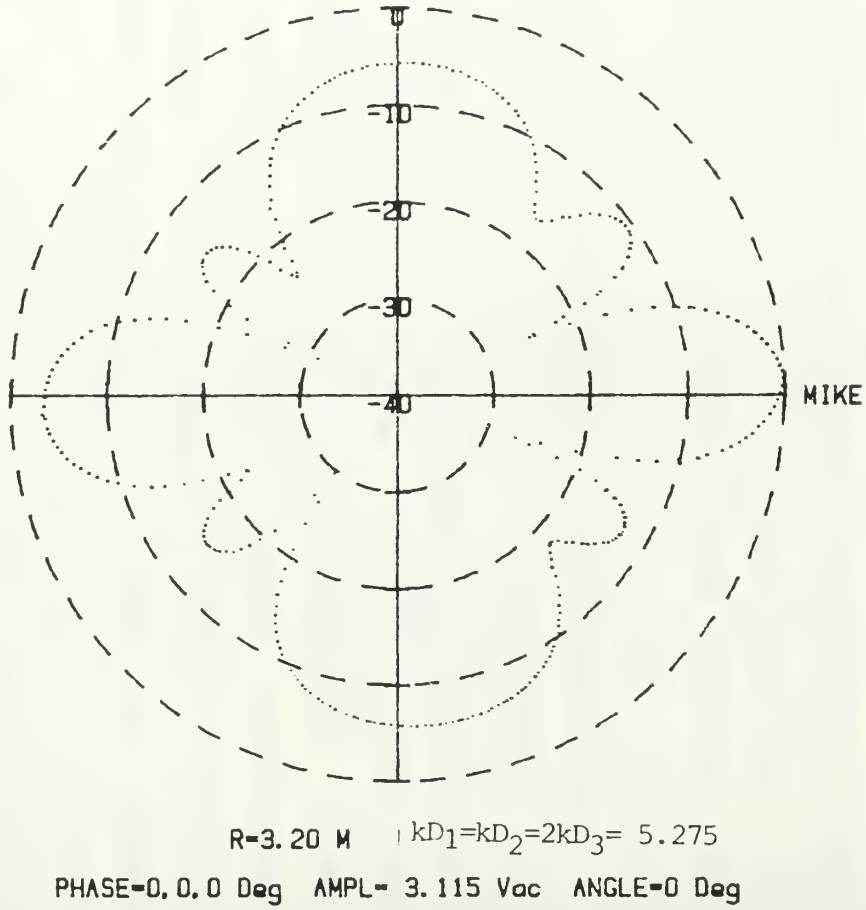

Figure 4.7 Laboratory Three Element Isosceles Plot

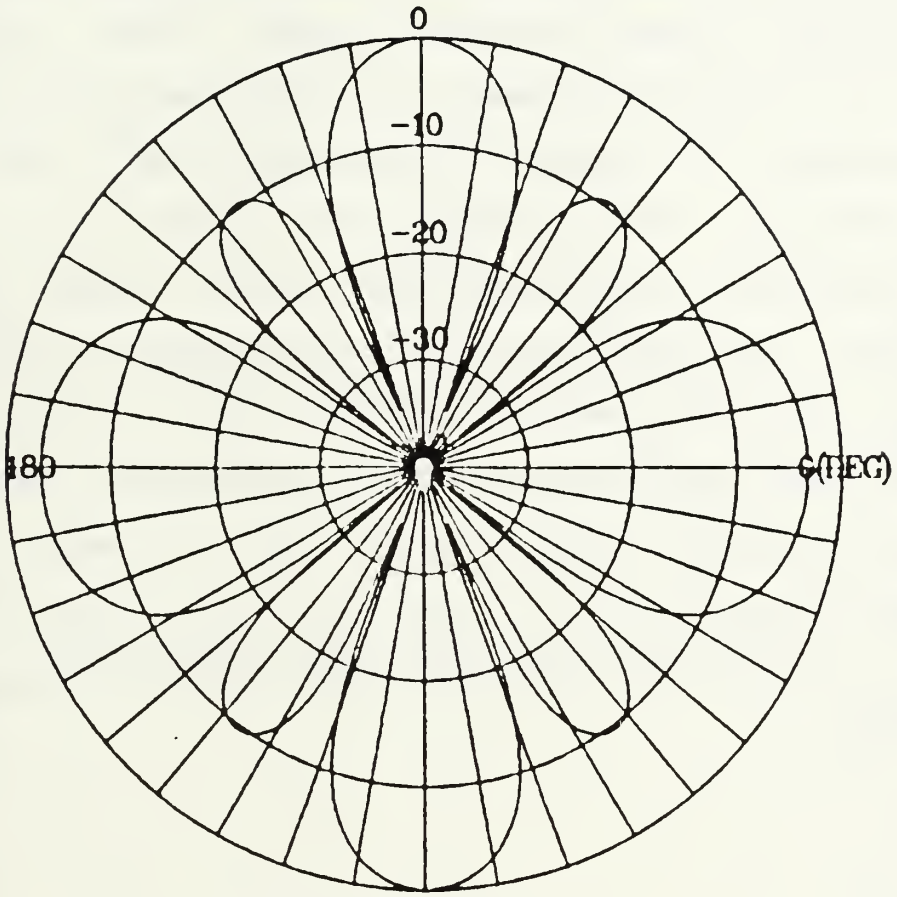

Figure 4.8 Three Element Isosceles Plot

in the equal amplitude shading, a small amount of scatter from the large array center joint, and a slight directionality of the individual acoustic drivers.

The beam patterns of a triplet in the form of an isosceles triangle are shown in Figs. (4.9), (4.10), and (4.11) to show the effects of tilting the array out of the horizontal to angles of theta equal to 30°, 60° and 90° respectively. The plane of the elements was initially perpendicular to the x-y plane, making theta, the angle between the z-axis and the array plane equal to 0°. The array plane was then tilted 30° about the x-axis and rotated 360° about the z-axis to obtain the data for Fig. (4.9). The array plane was then tilted in 30 increments to obtain Figs. (4.10) and (4.11). For this triplet case, $kD_1 = kD_2 = 2kD_3 = 5.28$ with kD3 sensing the elevation change (Fig. (4.12)).

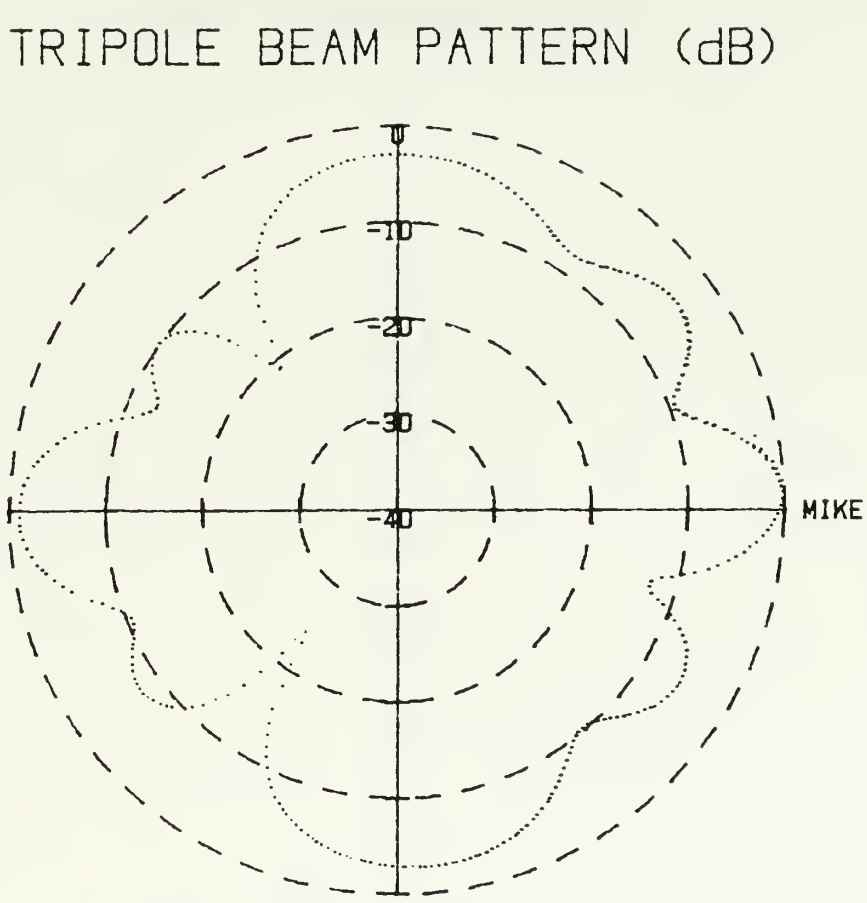

Figure 4.9 Beam Pattern for 30^{O} Tilt in Theta

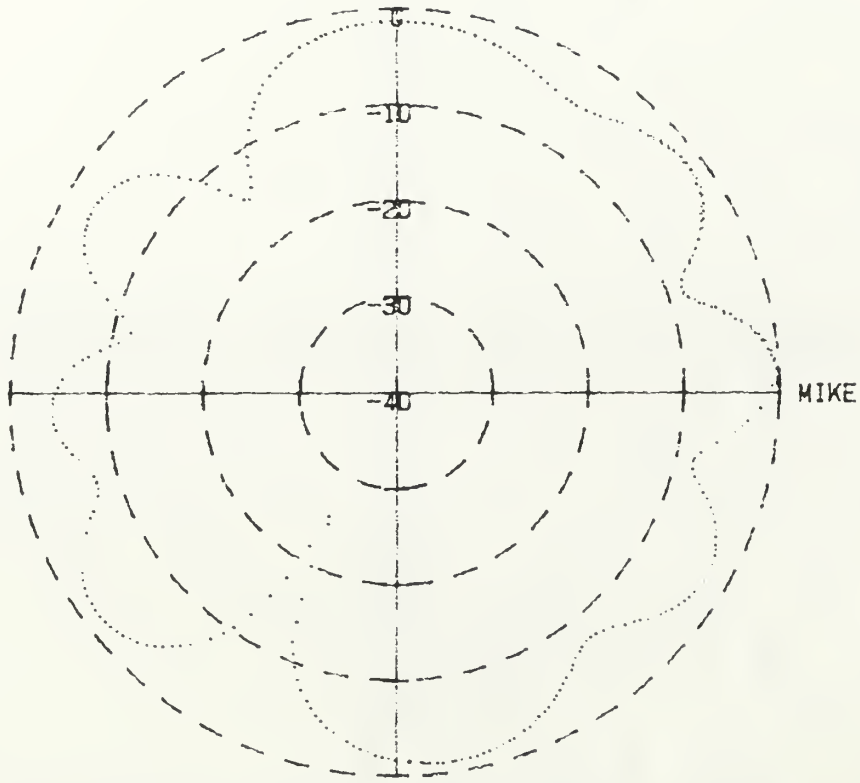

Figure 4.10 Beam Pattern for 60° Tilt in Theta

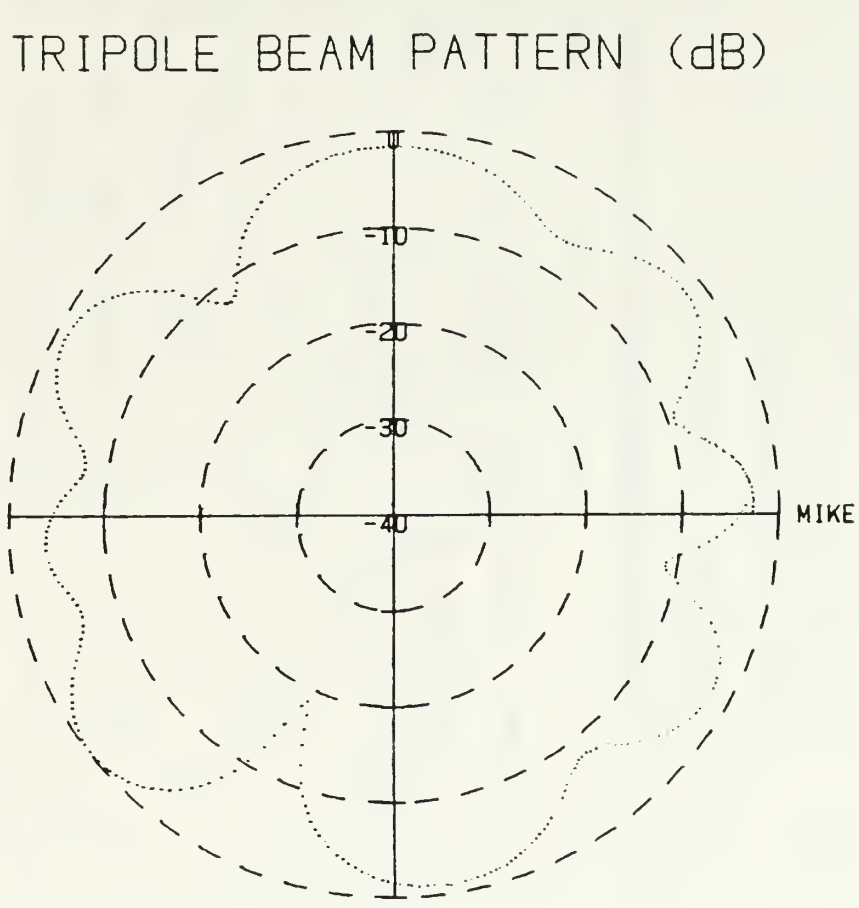

Figure 4.11 Beam Pattern for 90^{O} Tilt in Theta

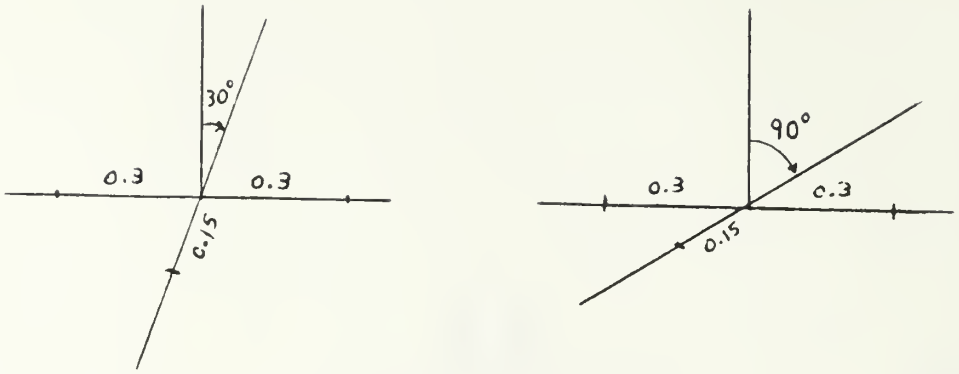

Figure 4.12 Array Configuration for Tilt Theta

These variations in tilt angle (theta) show that the 30° tilt has a diminished dB level for all lobes except the broad lobe coming into and exiting broadside. This is due, in large part, to the directionality of the drivers, because they are facing the microphone to a greater extent at 30° than at 90° of tilt and mutual shading exists. Additionally, for these various tilt angles, the Z-axis is rotating about the local vertical, as explained in section D of this chapter.

The last major configuration investigated was the quadruplet. It was looked at both as an axial quadruplet, Fig. (2.5), and as a planar array, Fig. (2.7). An experimental beam pattern for a planar array quadruplet with $kD_1 = kD2 = kD3 = kD4 = 5.26$ and all elements in phase is

shown in Fig. (4.13) along with a theoretical beam pattern, Fig. (4.14). There is good agreement between the two plots.

A plot of an axial quadruplet represented by an amplitude shaded triplet, obtained in the laboratory is shown in Fig. (4.15). Comparing Fig. (4.15) to Fig. (4.13), it is seen that when two elements of the planar array are in line, the arrival from the more distant source is weakened by the shadowing effect of the nearer source. Therefore, the near source can be emphasised by as much as one dB when compared to the far source. Additional plots of various configurations are contained in Appendix C, where good agreement continues to be seen.

D. EFFECTS OF ARRAY TILT, THETA

Referring back to Fig. (4.2), it is again noted that contour lines are directly related to polar plots when either theta or psi is fixed. However, the countour representation is not as useful when theta and psi are both changing with rotation of the array as in the case where the array has been tilted in theta. In this case the polar curve is found by superimposing a trajectory which is the specific locus of Θ and Ψ in the $\Theta - \Psi$ plane onto the contoured surface.

For this work, the microphone was fixed in the far field at a distance of 3.2 meters and level with the center joint of the array. Tilting the array in angle theta caused an

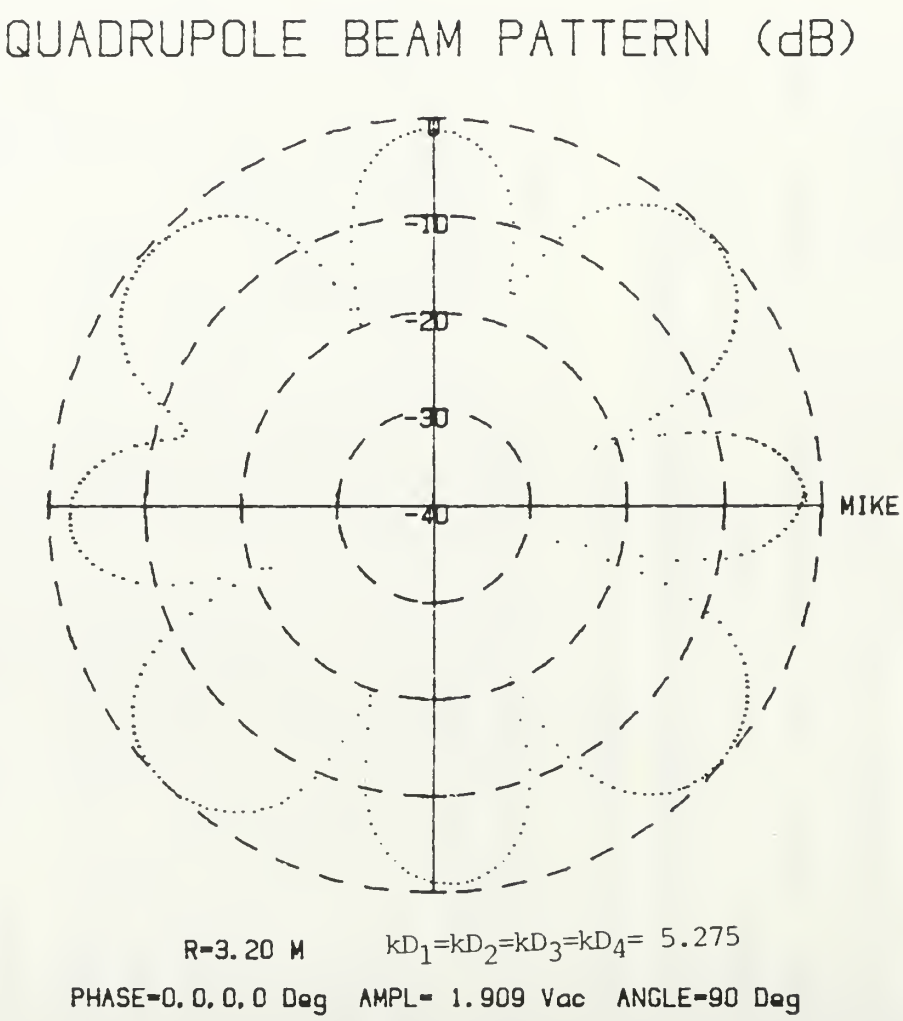

Figure 4.13 Laboratory Planar Quadruplet Plot

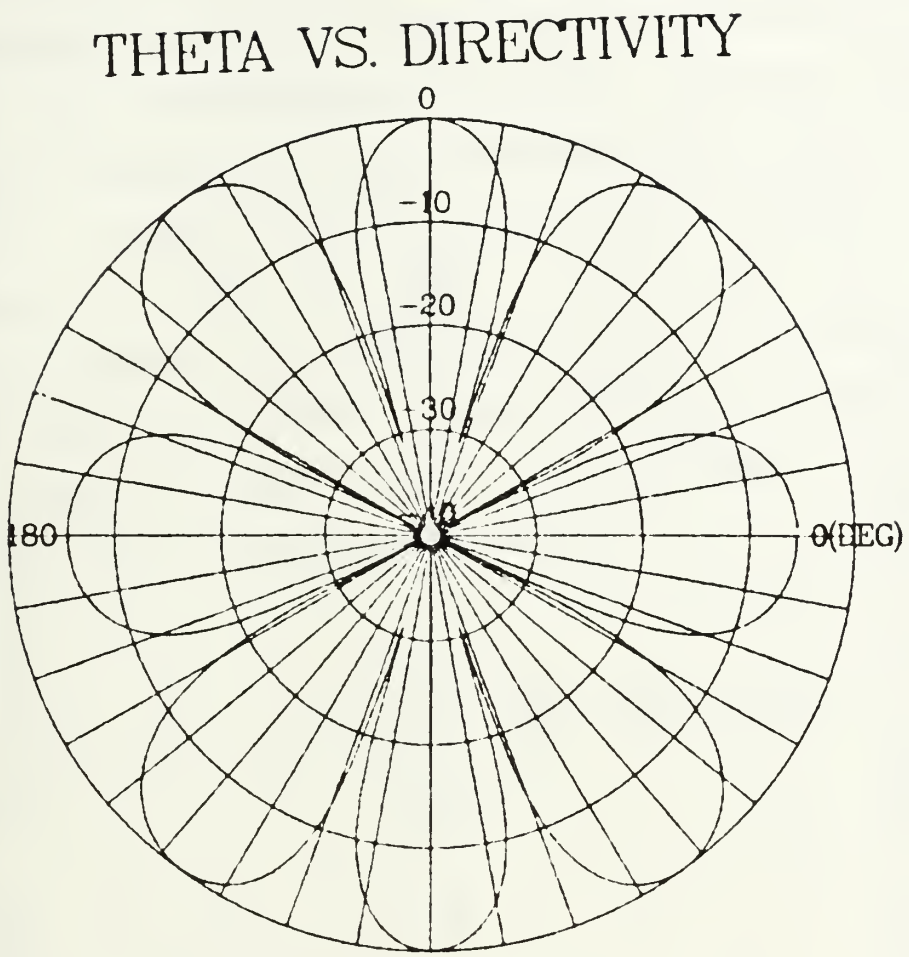

Figure 4.14 Theoretical Planar Quadruplet Plot

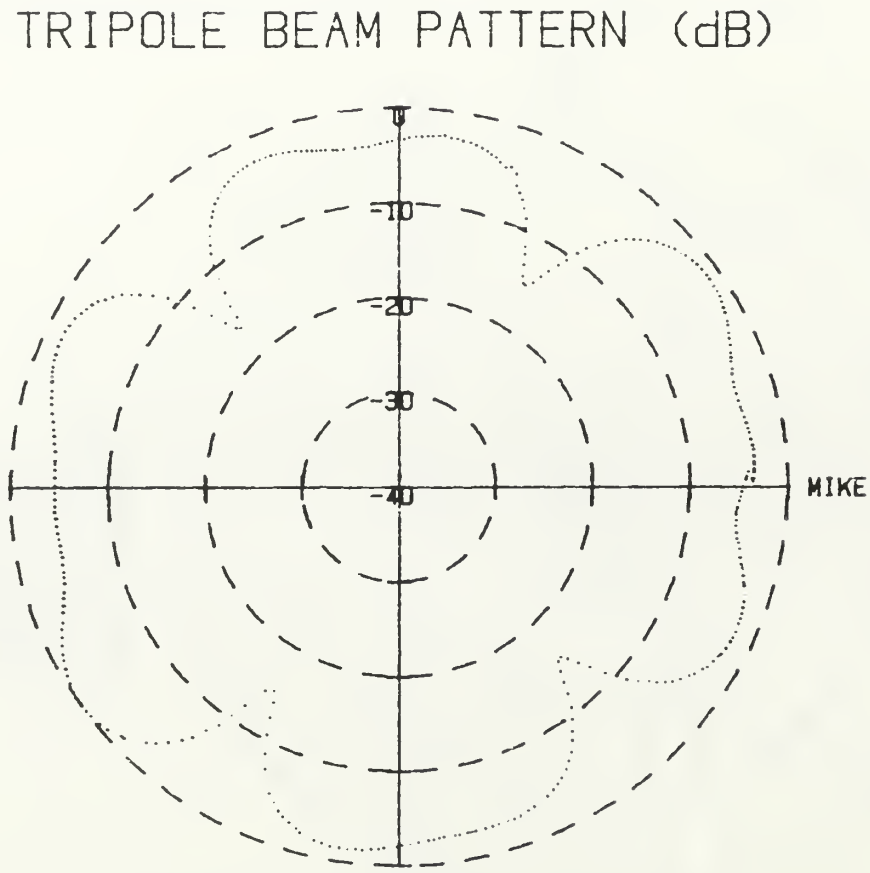

Figure 4.15 Laboratory Axial Quadrupole

offset between the Z-axis and the local vertical about which the array rotated. This can be seen in Fig. (4.16). In the left sketch, the array elements are aligned in the standard rectangular coordinate system, with the elements in the x-y plane and rotating about the z-axis. However, when the plane of the array is tilted 30° about the x-axis, $Y' = Y+30^{\circ}$ and $z' = z+30^{\circ}$. A 90° rotation about the z-axis to 270° yields $z' = 90^{\circ} - 30^{\circ} = 60^{\circ}$. This means that a 360° rotation about the z-axis causes Y1 and Z1 to vary from 120° to 60° and back to 120°. This is due to the fact that the microphone is fixed in space in the far-field rather than tilting with the plane of the array.

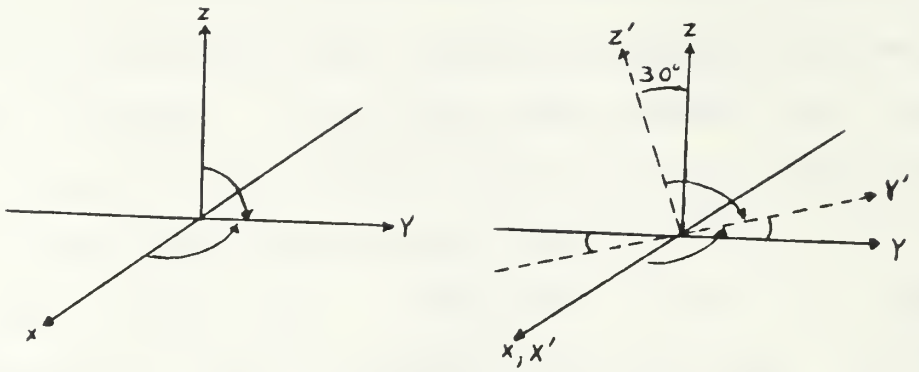

Figure 4.16 Z-axis Offset Effects

This problem does not occur in the classical representation where the microphone is fixed with respect to the axis of rotation of the array.

E. ERRORS

The sources of errors in the beam pattern measuring system were examined both mathematically and empirically. Sources of error for direct error analysis were based on multimeter values and power amplifier settings. With output reading from the multimeters and power amplifier exhibiting precision to the third decimal place, instrumentation errors from these sources are less than 1% and are not major contributing errors to measured beam patterns.

The major source of error in the system was determined empirically to be the acoustic driver positioning on the array. The effects of a small change in kd are shown in Figs. (4.17), (4.18), and (4.19). Here, it is seen that small changes in kD_i prove to have a large effect on the size of the small lobe at $\pm 90^{\circ}$ and 0° and 180°, thus yielding the largest error. A change of ± 5% in kd effected the structure by up to 6 dB as seen from the behavior of the small lobe at $\pm 90^{\circ}$. This change relates to a positioning error of about ± 3 centimeters and presented a small problem with respect to exact positioning of the speakers.

F. VALIDATION OF RESULTS

The laboratory beam patterns prove to be in good agreement with theoretical beam patterns. Small uniform beam pattern amplitude differences are merely a consequence of the difference in normalization methods employed in the theoretical and experimental beam pattern processing. The theoretical program normalized the directivity to the sum of the amplitude weights, whereas the laboratory program normalized the beam pattern to the highest received voltage.

An independent verification of the experimental program was performed by a thesis group under the auspices of Professor Don Walters of the Naval Postgraduate School Physics Department, who asked to use this experimental

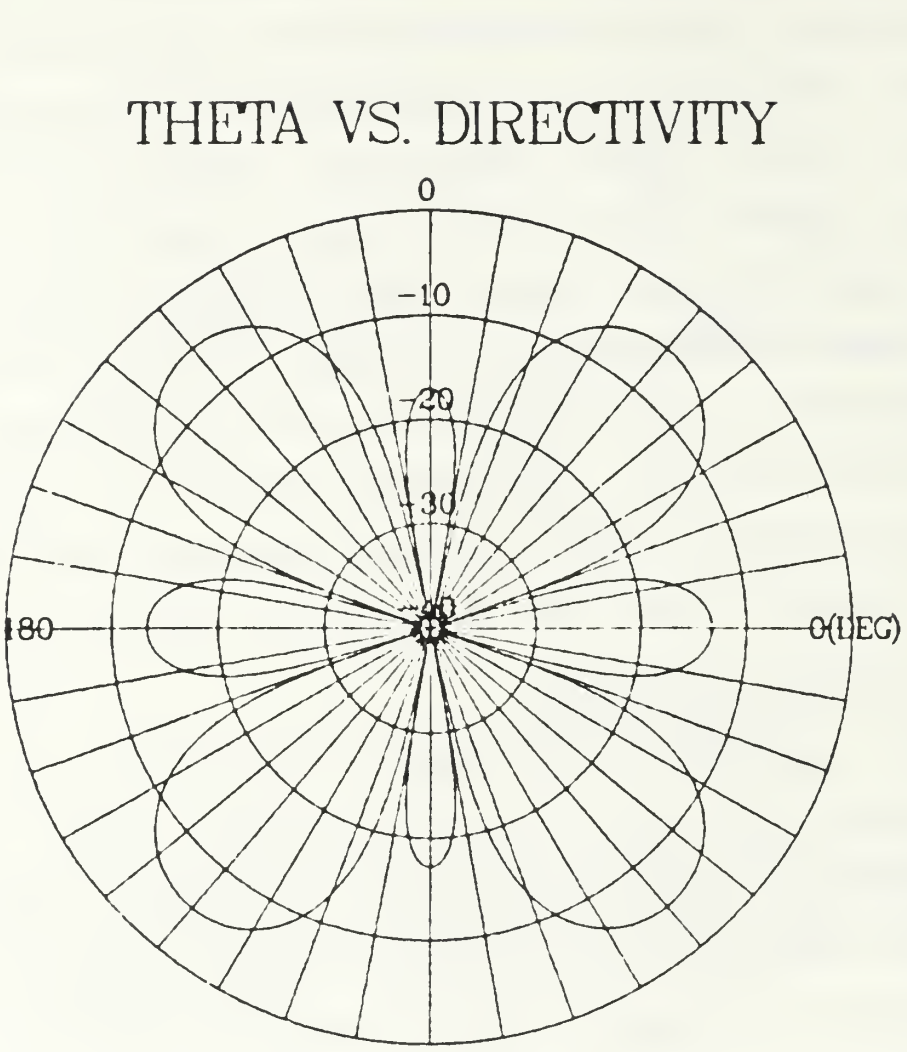

Figure 4.17 kD_i= 4.75 for Error Computation

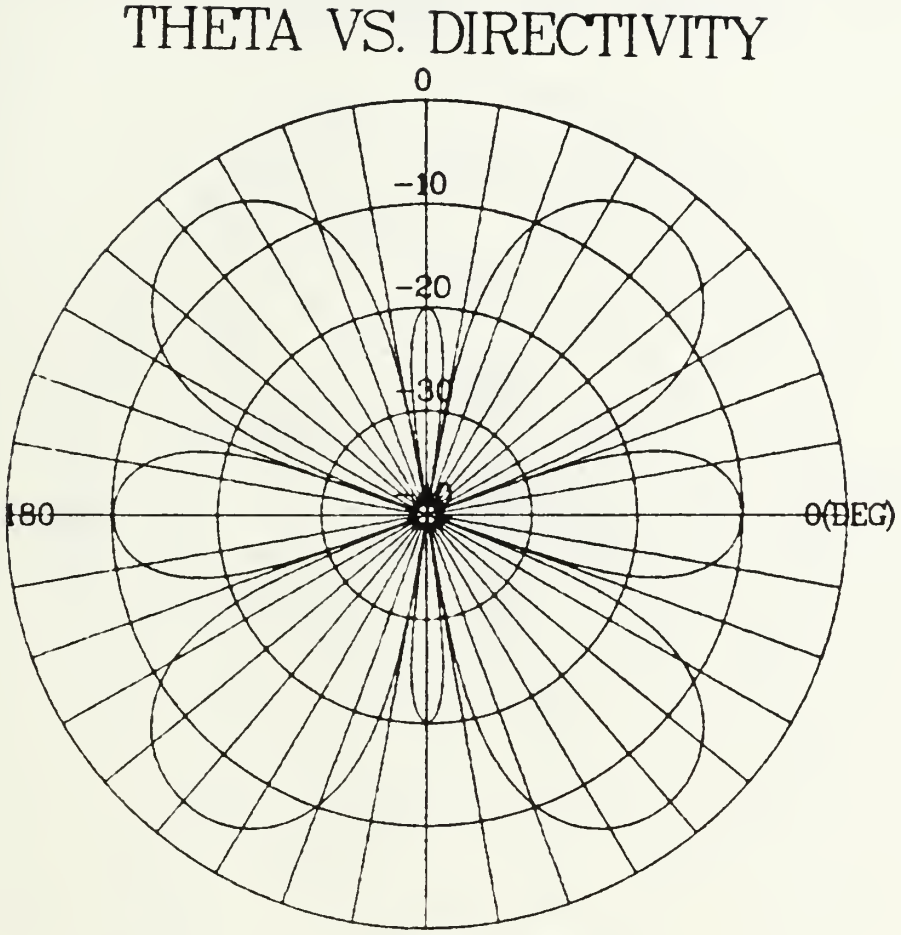

PHI= 60 DEGREE
$kD_1=kD_2=kD_3=kD_4$= 5.0
D1=0.5 D2=0.5
D3=0.5 D4=0.5
P2= 0 P3= 0 P4= 0
A=1. B=1. C=1.

Figure 4.18 kD_i= 5.0 for Error Computation

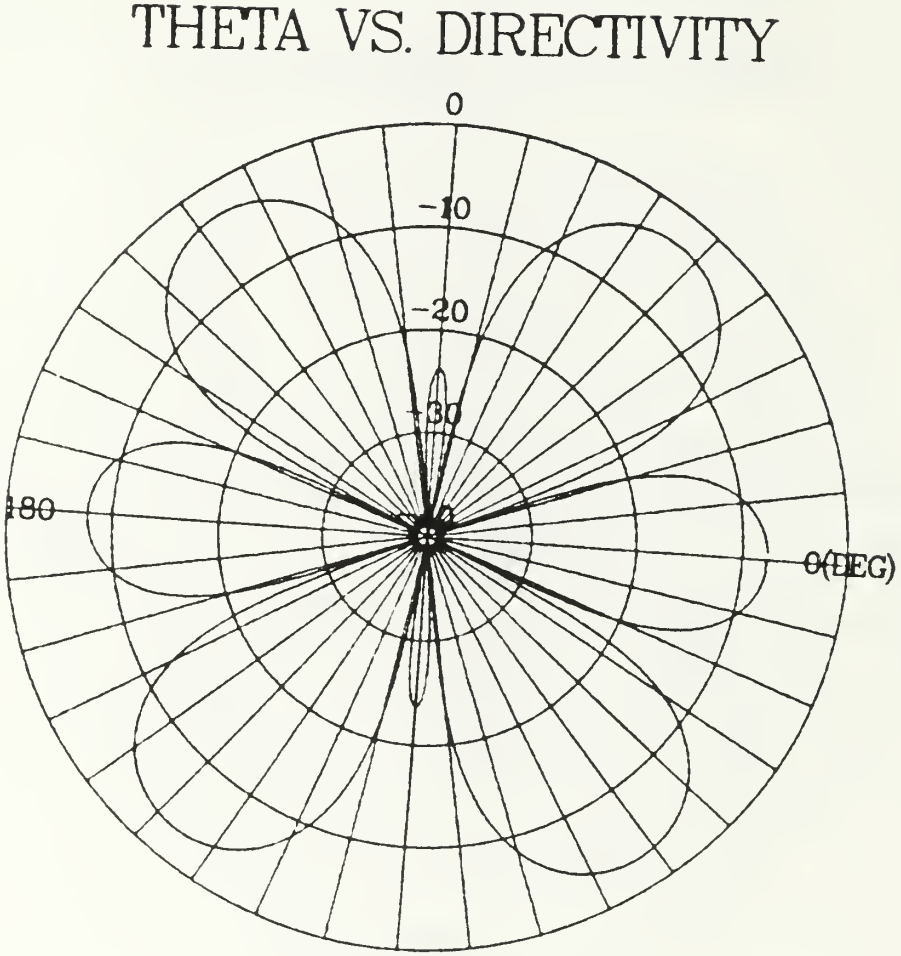

Figure 4.19 kD_i= 5.25 for Error Computation

system for related work. The laboratory system was placed in use by this research group in the selection of drivers for a 5 x 5 array currently under investigation and will be further utilized to establish beam patterns for this array.

TABLE II

ARRAY CONFIGURATIONS

Run No/ No. Elements	Freq (Hz)	Phase (deg)	Tilt (deg)	Amplitude Shading (VAC)	Spacing from Center (CM)
1	300		0		
1	300		45		
1	300		90		
1	960		0		
1	960		45		
1	960		90		
2	300	0,0	0		30
2	300	0,180	0		30
2	960	0,0	0		30
2	960	0,180	0		30
2	960	0,0	90		30
2	960	0,180	90		30
2	300	0,0	90		30
2	300	0,180	90		30
2	300	0,0	45		30
2	300	0,180	45		30
2	960	0,0	45		30
2	960	0,180	45		30
4	960	0,0,0,0	0		30
4	300	0,0,0,0	0		30
4	960	0,180,0,180	0		30
4	300	0,180,0,180	0		30
4	960	0,0,0,0	30		30
4	300	0,0,0,0	30		30
Quad11/4	300	0,180,0,180	30		30
Quad12/4	300	0,180,0,180	60		30
Quad13/4	960	0,180,0,180	60		30
Quad14/4	960	0,0,0,0	60		30
Quad15/4	300	0,0,0,0	60		30
Quad16/4	960	0,0,0,0	90		30
Quad17/4	960	0,180,0,180	90		30
Quad18/4	960	0,180,0,0	0		30,30,30,0
Tri1/3	960	0,0,0	0		30
Tri2/3	300	0,0,0	0		30
Tri3/3	300	0,180,0	0		30
Tri4/3	960	0,180,0	0		30
Tri5/3	960	0,0,180	0		30
Tri6/3	960	0,0,180	30		30
Tri7/3	960	0,180,0	30		30
Tri8/3	960	0,0,0	30		30
Tri9/3	960	0,0,0	30		30,15,30
Tri10/3	960	0,0,0	0		30.15.30
Tri11/3	960	0,180,0	0		30,15,30
Tri12/3	960	0,180,0	30		30,15,30
Tri131/3	960	0,180,0	60		30,15,30
Tri14/3	960	0,0,0	60		30,15,30
Tri15/3	300	0,0,0	60		30,15,30
Tri16/3	960	0,0,0	90		30,15,30
Tri17/3	960	0,180,0	90		30,15,30
Tri18/3	960	0,0,180	90		30,15,30
Tri20/3	960	0,0,0	0	1,1,1	30,0,30
Tri21/3	960	0,180,0	0	1,1,1	30,0,30
Tri22/3	960	0,0,0	0	1,2,1	30,0,30
Tri23/3	960	0,180,0	0	1,2,1	30,0,30
Tri24/3	960	0,0,180	0	1,2,1	30,0,30
Tri25/3	960	0,0,0	0	1,2,1	30,30,30
Tri26/3	960	0,0,0	30	1,2,1	30,30,30
Tri27/3	960	0,0,0	60	1,2,1	30,30,30
Tri28/3	960	0,0,0	90	1,2,1	30,30,30
Tri30/3	960	0,0,0	90	1,4,1	30,30,30
Tri31/3	960	0,180,0	90	1,4,1	30,30,30
Tri32/3	960	0,0,0	0	1,2,1	20,20,20
Tri33/3	960	0,180,0	0	1,2,1	20,20,20
Tri34/3	960	0,180,0	0	1,2,1	20,10,20
Tri36/3	960	0,0,0	0	1,2,1	20,10,20
Tri37/3	960	0,0,0	0	1,2,1	10,10,10
Tri38/3	960	0,180,0	0	1,2,1	10,10,10
Tri39/3	960	0,180,0	90	1,1,1	20,30,20
Tri40/3	960	0,180,0	90	1,2,1	17.9,17.9,17.9
Tri41/3	960	0,0,0	90	1,2,1	17.9,17.9,17.9
Tri43/3	960	0,0,0	90	1,2,1	26.8,26.8,26.8
Tri44/3	960	0,180,0	90	1,2,1	26.8,26.8,26.8

Note: (1) Additional data runs were made in some of the same configurations with fiberglass wrapped around the centerpiece to identify the effects of scattering.

(2) Additional data runs were made in some of the same configurations to verify repeatability.

V. CONCLUSIONS AND RECOMMENDATIONS

The doublet forms the basis for countless sonar and radar arrays currently utilized in both military and civilian applications. It is the ability to control the amplitudes and phases of the element of an array which allows the tailoring of the array radiation pattern to achieve the desired element of interest and promotes the maximization of array performance by increasing signal, decreasing noise or both.

The ability to rapidly measure the beam pattern of an array with complete confidence in the results is the basis behind this study. A laboratory system was developed to allow collection of a 360 point beam pattern in a 45 to 50 minute period. Software is easily modified to allow for collection of more or less than 360 data points. One of the major advantages of the computer-controlled method of obtaining a beam pattern is the relatively small amount of time required to achieve an accurate beam pattern based on a large data base.

Recommendations for improving the current laboratory system are based on reducing electrical noise of the rotation motor and reducing the size and weight of the array. First, the noise of the rotation motor prohibits continuous rotation while reading the resistance on the

potentiometer. Since a CW signal does not require broadband detection, filtering could be accomplished by use of a lock-in, fast fourier transform or heterodyne filter. Second, the array weight should be reduced to lessen the drag on the rotation motor and to reduce the amount of coast-down time required for heavier arrays. Next, the array center joint should be reduced in size to lessen any shadowing effects from the large, metal center joint. (Scattering effects seemed to be small judging from the lack of any effect on the polar plots when this joint was wrapped in fiberglass.) Also, driver mounts need to be designed so that the center of the driver face is directly on the axis. The 2 centimeter offset utilized for this investigation was minimized by making all readings in the far field. Last, greater distance between the driver and microphone would also help to lessen the 1 dB variation seen when an array was in an endfire orientation. This only affected the depth of the nulls.

APPENDIX A

EQUIPMENT DESCRIPTION

1. ANECHOIC CHAMBER

All experimentation was conducted in the anechoic chamber, Room Ø19, Spanagel Hall, Naval Postgraduate School. The anechoic chamber is a 99% echo free enclosure for sounds above 1ØØ Hertz. Acoustics research can be conducted on sound sources, receivers and scatterers with minimal interference from surface reflections or external noises. The size of the outer room in which the anechoic chamber floats is 37 feet x 24 feet x 21 feet high. Noise transmission from outside is minimized by the floating room within a room construction. The outer 12 inch concrete-walled room is separated from the inner room of concrete-block sides and floor by a 2 inch blanket of fiberglass or cork. Forty inch fiberglass wedges are attached to all surfaces of the inner room. These are designed to trap and absorb sounds which are incident upon them. A suspended floor is constructed of a grid of 225 wire cables, each stretched at a tension of 15Ø to 2ØØ pounds.

2. HP-86B PERSONAL COMPUTER

The HP-86B computer, operating in Hewlett-Packard BASIC language, is equipped with a 64 Kilobyte (K-byte) memory

with two additional 128 K-byte memory modules. The system proved more than sufficient for both program development and as an instrument controller. Instrument control by means of the computer was accomplished with the HP-IB (Hewlett-Packard Interface Bus) which is a standard connection on most HP equipment. This facilitated instrument control for the various system components.

3. HP 7470A GRAPHICS PLOTTER

The HP 7470A Graphics Plotter is a vector plotter which utilizes HP's micro-grip drive technology, moving both the paper and the pen. Multicolor plotting is available, but there are only two pen positions so pauses must be used to change pen colors. Only one line of program code is required to shift the output to and from the plotter to the HP-86B CRT.

4. HP-4192A LOW FREQUENCY IMPEDANCE ANALYZER

The HP-4192A LF Impedance Analyzer is a fully automated instrument designed to measure a large range of impedance related characteristics. It can be used to measure eleven impedance parameters: absolute value of impedance Z, absolute value of admittance Y, phase angle Θ, resistance R, reactance X, conductance G, susceptance B, inductance L, capacitance C, dissipation factor D, and quality factor Q. The HP-4192A was used to measure the frequence response,

impedance, resistance and reactance of the University Sound ID-30 driver units as discussed in section 10 of this appendix.

5. HP-3421A DATA ACQUISITION/CONTROL UNIT

The HP-3421A Data Acquisition/Control Unit (DAC) has a 5.5 digit voltmeter, a 10 kHz counter and an HP-IB controller interface. The DAC was utilized as a computer controlled switching unit with channels 1 and 2 configured as actuators. This provided a voltage path to control relays in the motor power and direction controller for rotation of the ID-30 speaker array, Fig. (A.1).

6. HP-3478A MULTIMETER

The HP-3478A Multimeter provides both resistance and voltage measurement capabilities with 3.5 to 5.5 digit resolution with + 0.3 mV accuracy on the 100 Hz to 20 kHz scale. The multimeter was remotely controlled by the computer via the HP-IB. Voltage readings from the GR-1962 microphone and resistance readings from the variable potentiometer on the array rotator being read by the multimeter and then sent to the HP-86B computer via the HP-IB.

7. HP-3314A FUNCTION GENERATOR

The HP-3314A Function Generator is a multimode function generator which provides sine, square, and triangular

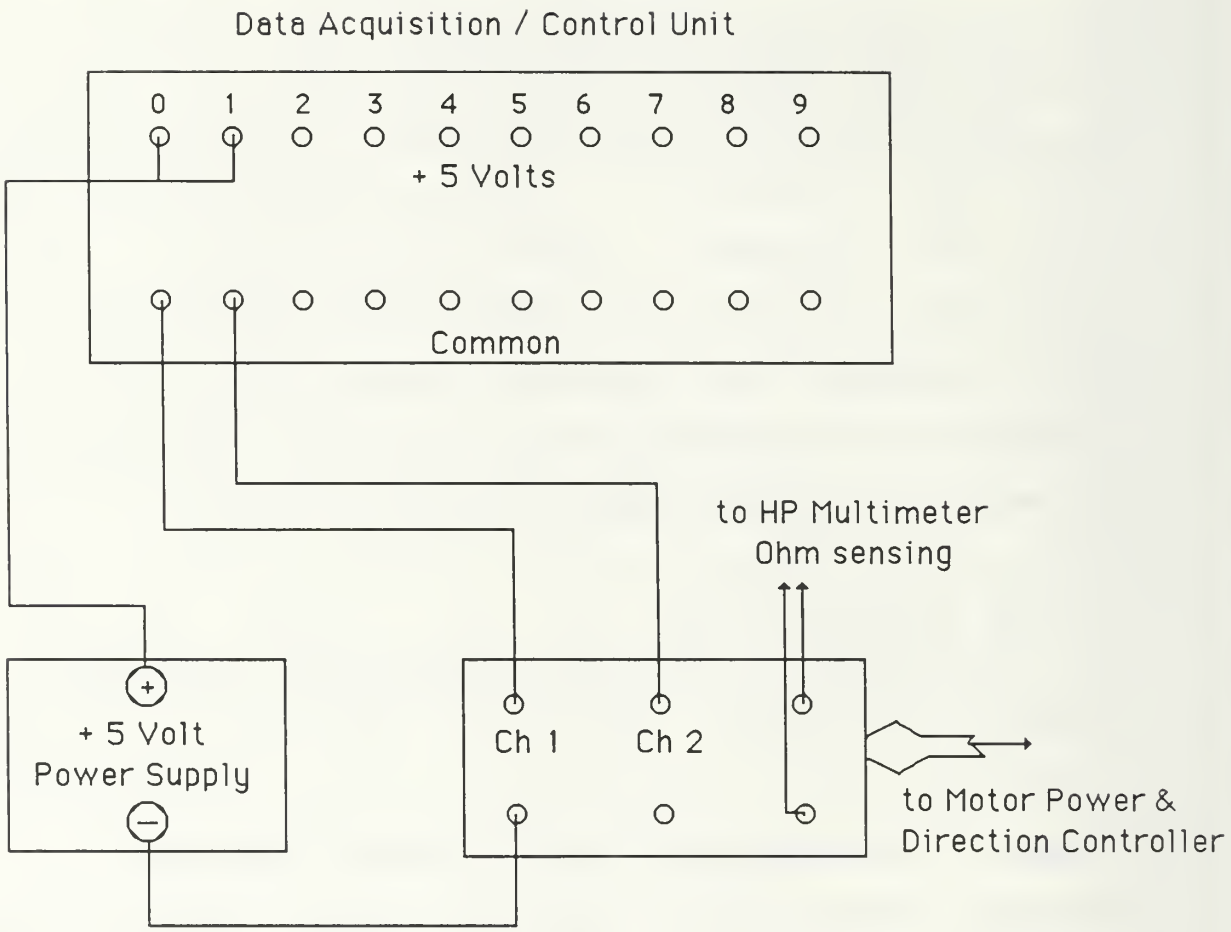

Figure A.1. Data acquisition connection to motor-power controller.

functions as well as any desired arbitrary wave form from frequencies of 0.001 Hz to 19.999 MHz. It was operated in the free run mode providing a continuous 1 Vac sine wave to Hp-467A Amplifier's inputs.

8. HP-465A AMPLIFIER

The HP-465A Amplifier is a general purpose preamplifier and impedance converter from 10 megohms to 50 ohms. It has a selectable gain of 20 or 40 decibels and is stable over a frequency range of 5 Hz to 1 MHz. The amplifier was used to amplify the received signal from the GR-1962 microphone.

9. HP-467A POWER AMPLIFIER

The HP-467A Power Amplifier is a 10 watt peak power amplifier and a -20 to +20 vold dc power supply. It has a wide band width with low dc drift from 5 Hz to 1 MHz. A variable gain control allows adjustments of gain between zero and 10 with resolution better than 0.1% of full power. Four HP-467A's, one for each ID-30 driver unit, were utilized in adjusting power inputs from the function generator.

10. UNIVERSITY SOUND ID-30 DRIVER UNITS

The University Sound ID-30's are medium power horn driver units designed specifically for wide midrange response. Their tropicalized voice coils are 2 inches in diameter with linen base molded phenolic diaphragms with a

minimal 16 ohm impedance. The frequency response is 85 Hz to 7.5 Khz. They were used as the sound sources.

11. GENERAL RADIO TYPE 1962 MICROPHONE

The GR-1962 microphone is a Ø.5 inch diameter electret condenser, microphone, providing a flat response at zero decibels between 2Ø Hz and 15 Khz. It experiences rapid drop off above 15 Khz and is nonresponsive above 21 Khz. A General Radio Model 156Ø-P62 inline power supply was connected to the microphone 156Ø-P42 preamplifier to amplify the received signal.

12. HP-6215A POWER SUPPLY

The HP-6215A power supply provides zero to 3Ø volts dc or Ø to 5ØØ Mamps. It was used to provide switching voltage for the Motor power relay in the direction controller.

13. MOTOR POWER AND DIRECTION CONTROLLER

The controller for the array rotator controlled power to the rotator and also the direction of rotation. With leads to the rotator assembly potentiometer, it also provided resistances which corresponded to a given angle (Ø to 1Ø Kohms translated into Ø to 36Ø degrees). A +5 volt dc signal to IC-1 via channel 1 of the DAC provided on/off power to the rotator and +5 Volts to IC-2 via channel zero of the DAC provided clockwise rotation of the driver assembly unit (Figure A.2). [Ref. 8]

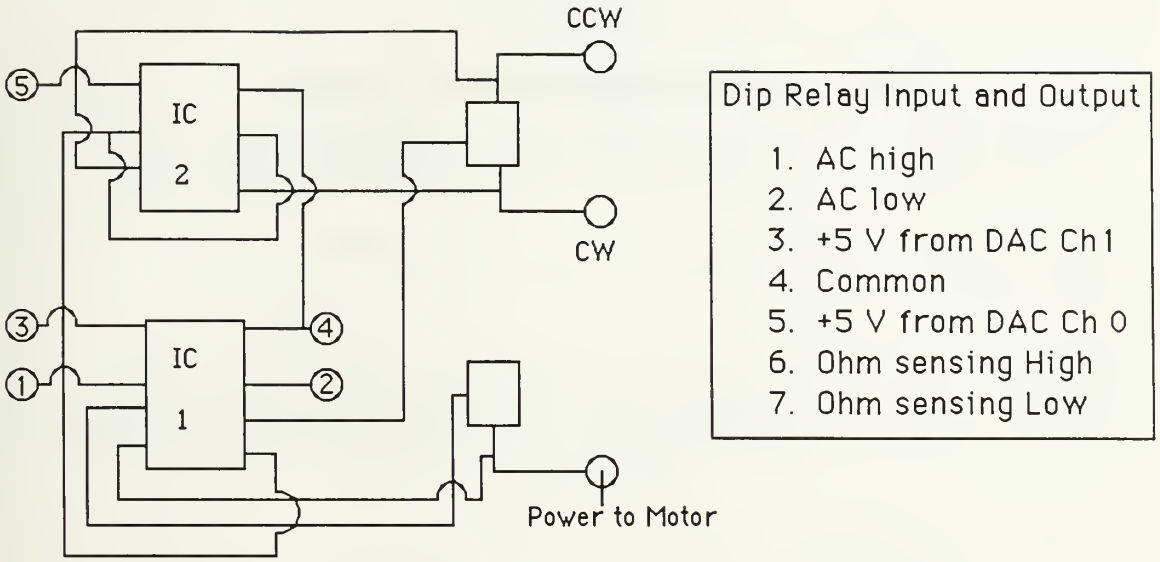

a) Circuit Diagram for Modified Motor Power and Direction Controller

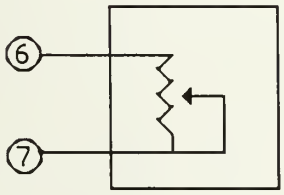

b) 360° / 10 kΩ Potentiometer

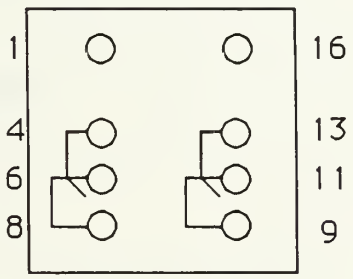

c) 16 Pin DIP Relay

Figure A.2. Circuit diagram for modified motor-power / direction controller [Ref. 9., p. 57].

APPENDİX B

BEAM PATTERN COMPUTATION AND PLOT PROGRAM

```
10 PRINT "***** BEAM PATTERN COMPUTATION AND PLOT PROGRAM *****"
11 PRINT "*************************************************"
12 !
13 !
20 PRINT "***** SET_UP *****"
21 !
22 !
30 PRINT CHR$ (10)
40 PRINT "THIS PROGRAM CONTROLS THE FOLLOWING APPARATUS TO MEASURE, DISPLAY,"
50 PRINT "PLOT AND STORE THE DIRECTIONAL CHARACTERISTICS OF A SINGLET,"
60 PRINT "DOUBLET, TRIPLET, AND QUADRUPLET ARRAY."
61 !
62 !
70 PRINT " INSTRUMENT                    ADDRESS "
80 PRINT " __________                    _______ "
90 PRINT " HP_3478 MULTIMETER (VOLTS)     724    "
100 PRINT " HP_3478 MULTIMETER (RES)       723    "
110 PRINT " DATA AQUISITION/CONTROL        709    "
111 !
120 DISP "INITIALIZE INSTRUMENTS"
121 !
130 REM *** PRESET AND INITIALIZE INSTRUMENTS***
140 OUTPUT 709 ;"RS" ! RESET
150 OUTPUT 723 ;"F3R5T1" ! FREE RUN 30KOHMS
160 OUTPUT 724 ;"F2RAT1" ! FREE RUN AUTORANGE AC VOLTS
161 !
170 DISP "INITIALIZE PROGRAM"
171 !
180 OPTION BASE 1
190 COM ANGLE(150),CALC_ANGLE(150),NAME$[80]
200 DEG
210 PRINTER IS 701
220 INTEGER I,C,L,N
230 DIM P(360),VOLT(360),OHMS_DATA(360),X(360),Y(360),K(360)
240 MVOLT=0
250 MASS STORAGE IS ":DATA1"
260 DISP "NUMBER OF DATA POINTS DESIRED?"
270 BEEP 10,300
280 INPUT N
290 DISP "WANT NEW DATA (Y/N)?"
300 BEEP 10,300
```

```
310 INPUT Q$
320 IF Q$="Y" THEN GOTO 350
330 IF Q$="N" THEN GOTO 780
340 GOTO 300
350 REM *** DEFAULT PARAMETERS ***
381 !
382 ! MUST INSERT FOR LINES 390, 400, 410 AND 810 PRIOR TO START OF RUN
383 !
390 CREATE "* INSERT NAME OF RUN *",360,16
400 ASSIGN# 1 TO  "* INSERT NAME OF RUN *"
410 NAME$="* INSERT NAME OF FILE *" ! FILE NAME
420 FULLSCALE=500 ! LOCK_IN MVAC
430 CONV=360/10000 ! CONVERT OHMS TO DEGREES
440 SET_UP: ! *** SET_UP MEASUREMENT PARAMETERS ***
450 PRINT CHR$ (10)
490 DISP "MANUALLY ENTER DESIRED FREQUENCY FOR SPEAKER DRIVER"
500 DISP "ENTER 0 IF NO CHANGE"
510 DISP "ENTER 1 TO CHANGE TITLE"
520 BEEP 10,600
530 INPUT C ! CHOICE
540 IF C=0 THEN GOTO 560
550 IF C=1 THEN GOTO 750
560 PRINT CHR$ (10)
570 OUTPUT 709 ;"CLS0" ! ROTATE CW
575 PRINT "I","OHMS_DATA (OHMS)","VOLT (VAC)"
580 FOR I=1 TO N
590 OUTPUT 709 ;"CLS1" ! POWER TO MOTOR ON
600 WAIT .5 ! MILLISECONDS
610 OUTPUT 709 ;"OPN1" ! POWER TO MOTOR OFF
620 WAIT 4000
630 ENTER 723 ; OHMS_DATA(I)
640 ENTER 724 ; VOLT(I)
650 PRINT I,OHMS_DATA(I),VOLT(I)
660 NEXT I
690 FOR I=1 TO N
700 PRINT# 1 ; OHMS_DATA(I),VOLT(I)
710 NEXT I
720 ASSIGN# 1 TO  *
730 GOSUB PLOT_ROUTINE
740 GOTO 770
750 ENTER NAME$ ! NEW TITLE$
760 GOTO 480
```

```
770 END
780 DISP "WHAT IS DATA RUN DESIRED?"
790 BEEP 10,500
810 ASSIGN# 1 TO  "* INSERT NAME OF RUN *"
820 FOR I=1 TO N
830 READ# 1 ; OHMS_DATA(I),VOLT(I)
840 NEXT I
850 ASSIGN# 1 TO  *
860 GOTO 730
861 !
862 !
870 PLOT_ROUTINE: ! *** PLOTS POLAR DATA ***
871 !
872 !
880 PLOTTER IS 705
890 GRAPH
900 CLEAR
910 PEN 1
920 SCALE  60,60,-60,60
930 XAXIS 0,10,-40,40
940 YAXIS 0,10,-40,40
950 CSIZE 3
960 LINE TYPE 1
970 FOR L=0 TO 40 STEP 10
980 MOVE 0,L
990 LORG 6
1000 LABEL L-40
1010 NEXT L
1020 LINE TYPE 1
1030 CSIZE 6
1040 MOVE 0,50
1041 !
1042 ! INSERT LABELS 1050, 1080 AND 1100 PRIOR TO START OF RUN
1043 !
1050 LABEL ;"QUADRUPOLE BEAM PATTERN (dB)"
1060 CSIZE 3
1070 MOVE 0, 45
1080 LABEL ;"R=3.20 M","    ","Id=3.30","    ","FREQ=300 Hz"
1090 MOVE 0,-50
1100 LABEL ;"PHASE=0,180,0,180 Deg","   ","AMPL= 0.093 Vac","   ","ANGLE=30 Deg"
1110 MOVE 45,0
1120 LORG 5
```

```
1130 LABEL ;"MIKE"
1140 LINE TYPE 4
1150 FOR L=10 TO 40 STEP 10
1160 MOVE L,0
1170 FOR I=0 TO 360 STEP 5
1180 DRAW L*COS (I),L*SIN (I)
1190 NEXT I
1200 NEXT L
1210 LINE TYPE 1
1220 PEN UP
1230 PEN 2
1240 FOR I=1 TO N ! BEGINS BEAM PATTERN COMPUTATION
1250 IF VOLT(I)>MVOLT THEN MVOLT=VOLT(I)
1260 NEXT I
1270 FOR I=1 TO N
1280 K=OHMS_DATA(I)/10000*360
1290 K1=K
1300 IF OHMS_DATA(I)<10 THEN K=K1+360/295
1310 IF OHMS_DATA(I)>10500 THEN GOTO 1400
1320 VECTOR=20*LGT (VOLT(I)/MVOLT)+40
1330 LINE TYPE 3
1340 IF VECTOR<1 THEN VECTOR=0
1350 PRINT I,K,VECTOR
1360 X(I)=VECTOR*COS (K)
1370 Y(I)=VECTOR*SIN (K)
1380 PLOT X(I),Y(I)
1390 PEN UP
1400 NEXT I
1410 RETURN
```

TABLE III

SAMPLE PROGRAM DATA COLLECTION OUTPUT

I	OHMS_DATA (OHMS)	VOLT (VAC)
1	4	.34224
2	23	.78029
3	36	.75382
4	56	.70283
5	79	.66387
6	106	.61826
7	128	.57768
8	150	.54098
9	194	.52056
10	215	.51957
11	251	.53613
12	281	.56734
13	308	.60786
14	330	.65774
15	369	.72735
16	401	.80824
17	429	.86951
18	458	.93089
19	488	1.00539
20	522	1.07149
21	543	1.12759
22	572	1.18977
23	600	1.244
24	628	1.28825
25	648	1.3225
26	673	1.36172
27	704	1.40042
28	726	1.42822
29	755	1.4564
30	786	1.47833
31	814	1.49626
32	846	1.50758
33	869	1.51187
34	895	1.51108
35	924	1.50482

TABLE IV

SAMPLE CALCULATED BEAM PATTERN OUTPUT

I	Degrees	Decibels
1	1.36433898305	31.8170537827
2	.823	34.2542573403
3	1.296	33.9544396328
4	2.016	33.3461423354
5	2.844	32.8507973877
6	3.816	32.2325595086
7	4.608	31.6428831572
8	5.76	31.0727607067
9	6.984	30.739552392
10	7.74	30.7220178563
11	9.036	30.9945387083
12	10.116	31.4860046043
13	11.088	32.0852078323
14	11.88	32.7702215971
15	13.284	33.6440053809
16	14.436	34.5384233377
17	15.444	35.1946281389
18	16.488	35.7871038167
19	17.568	36.4558277425
20	18.792	37.0089989818
21	19.640	37.4621633313
22	20.592	37.9183967977
23	21.6	38.3055441246
24	22.608	38.6091395402
25	23.328	38.8370501316
26	24.228	39.09089264
27	25.344	39.3343026072
28	26.136	39.5050387295
29	27.18	39.6747499227
30	28.296	39.8045643216
31	29.304	39.9092778386
32	30.456	39.9747438642
33	31.284	40
34	32.22	39.9948856871
35	33.264	39.95802761

APPENDIX C

Experimental and Theoretical Plots

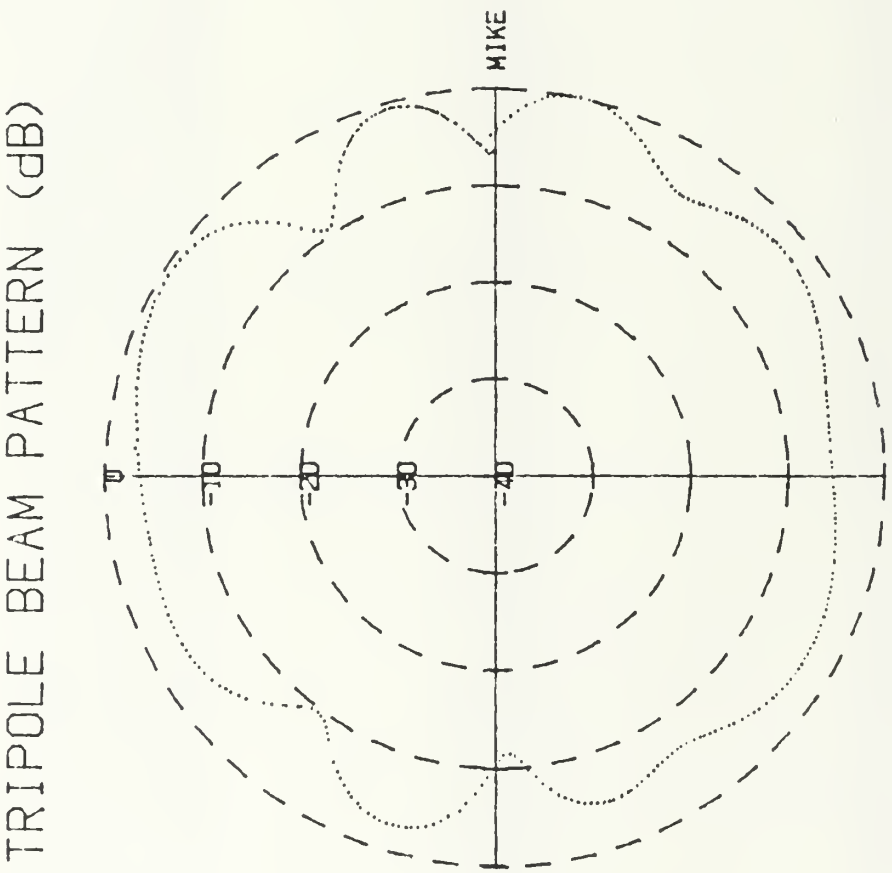

Figure C.1 Laboratory Three Element Isosceles Plot

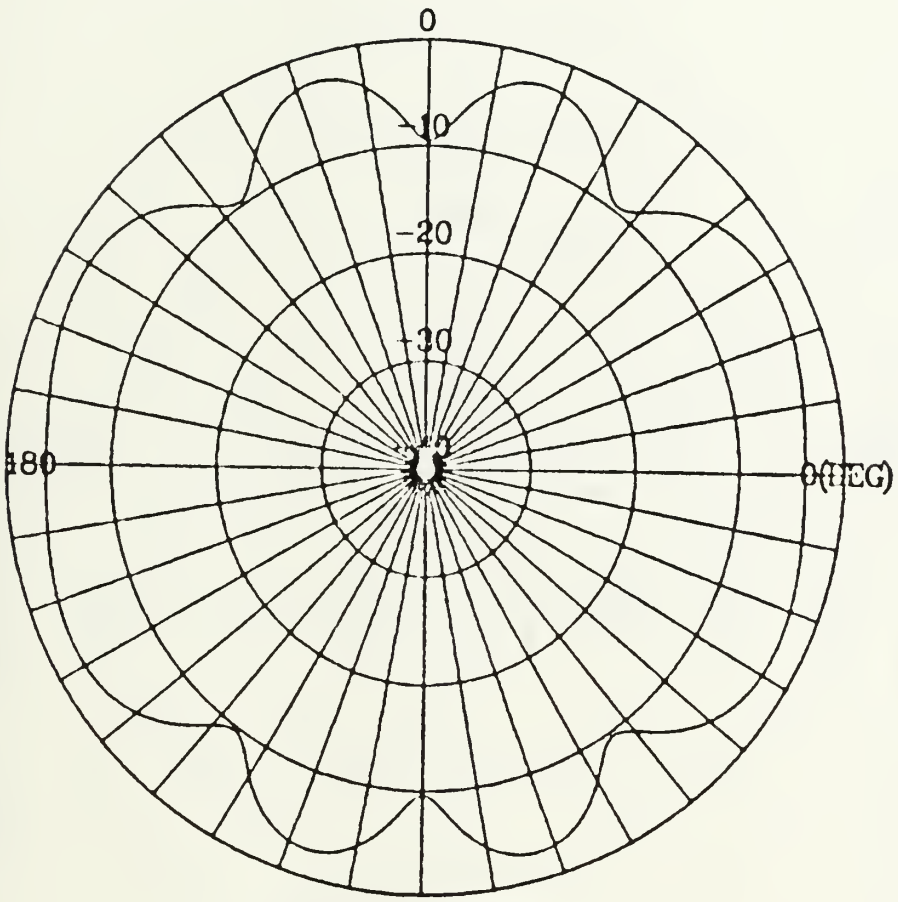

Figure C.2 Theoretical Three Element Isosceles Plot

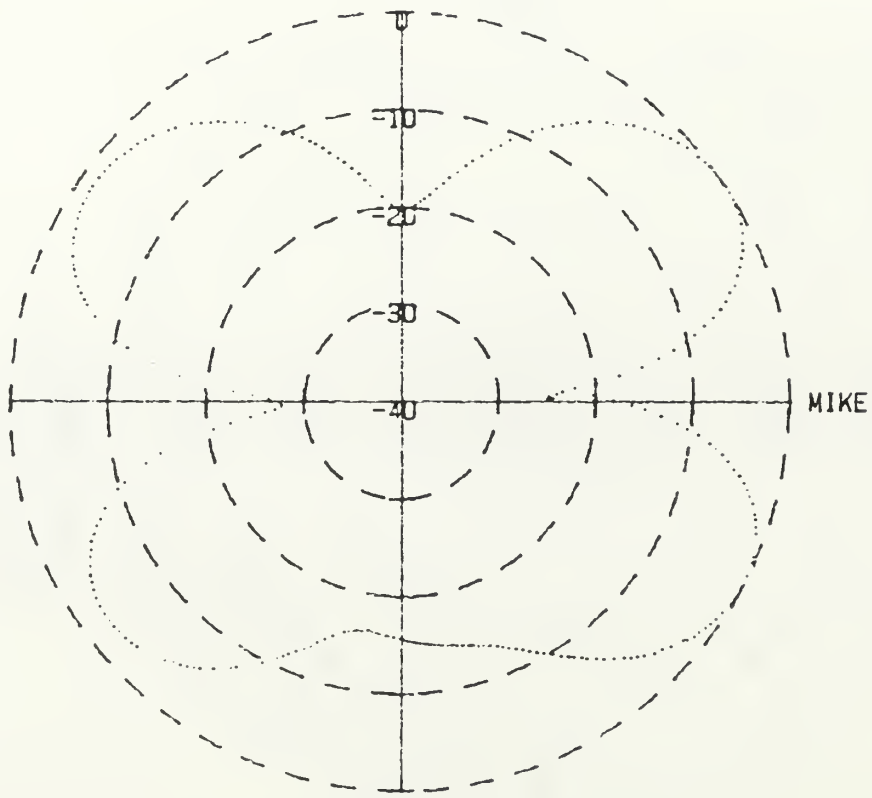

Figure C.3 Laboratory Planar Quadrupole Plot

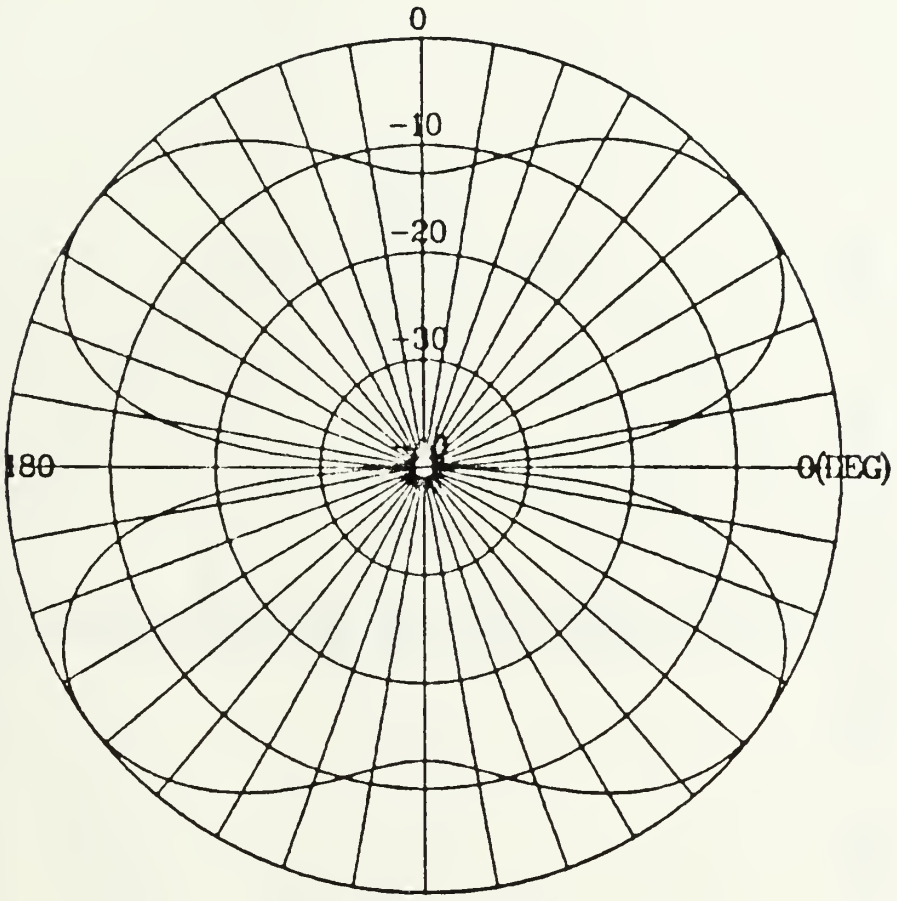

Figure C.4 Theoretical Planar Quadrupole Plot

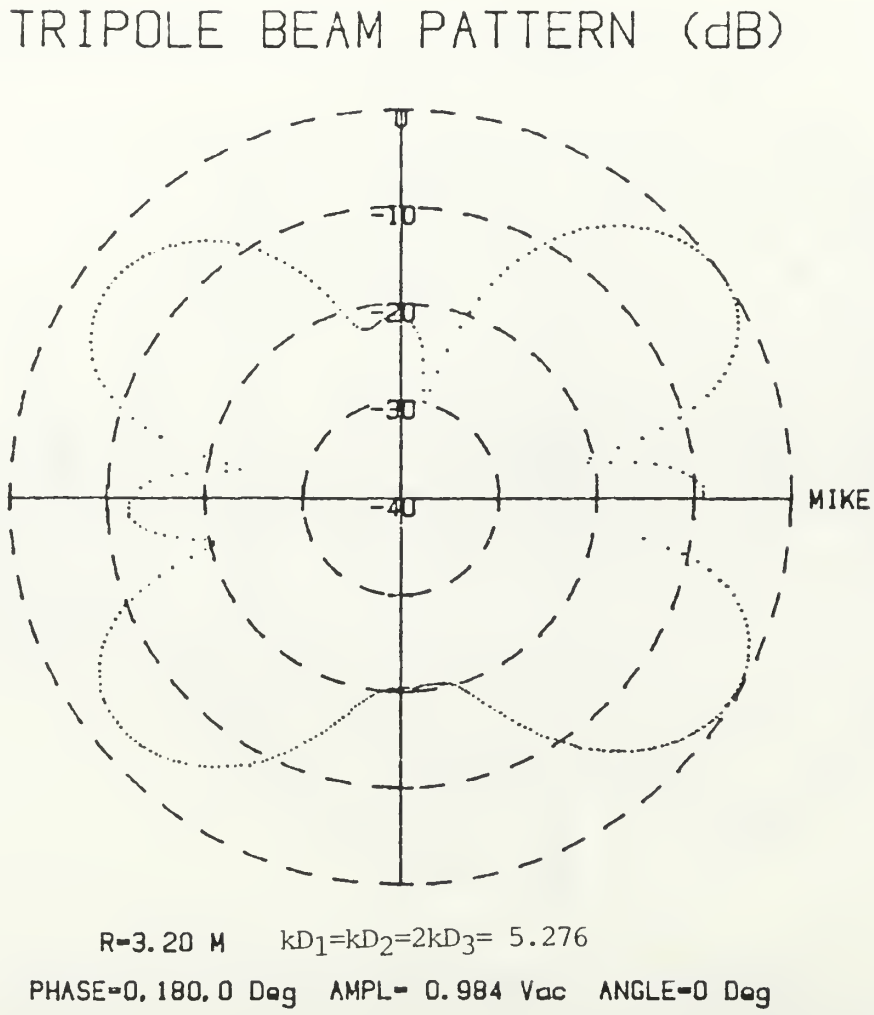

Figure C.5 Beam Pattern for 0^{O} Tilt in Theta (Tripole Isosceles)

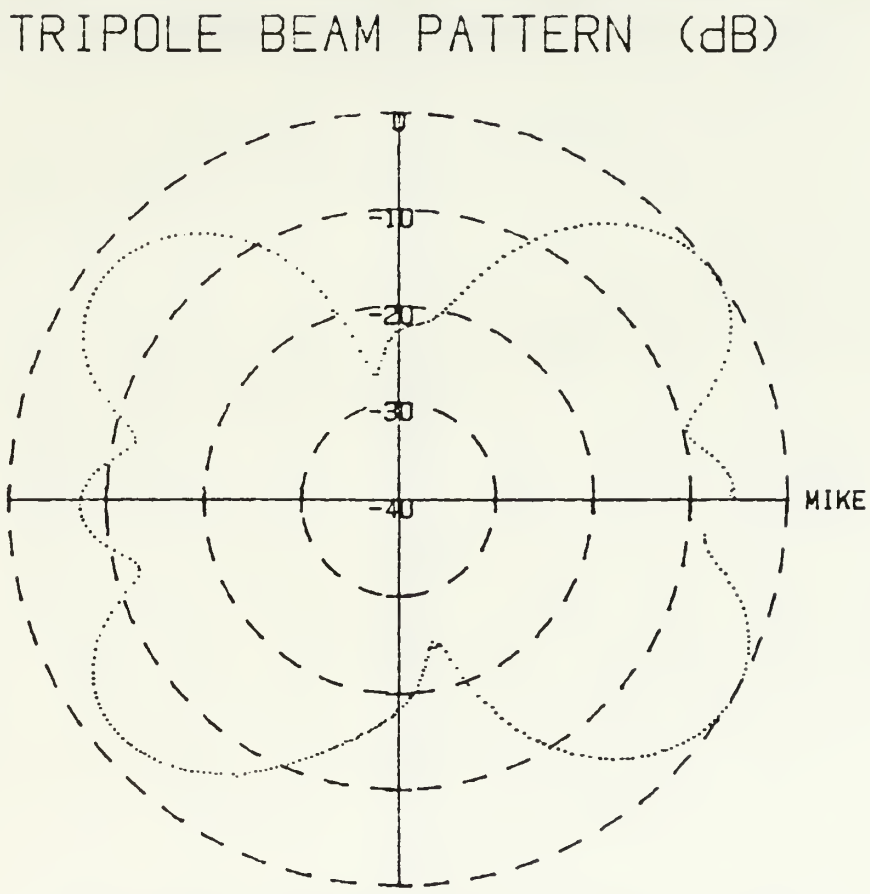

Figure C.6 Beam Pattern for 30^{O} Tilt in Theta (Tripole Isosceles)

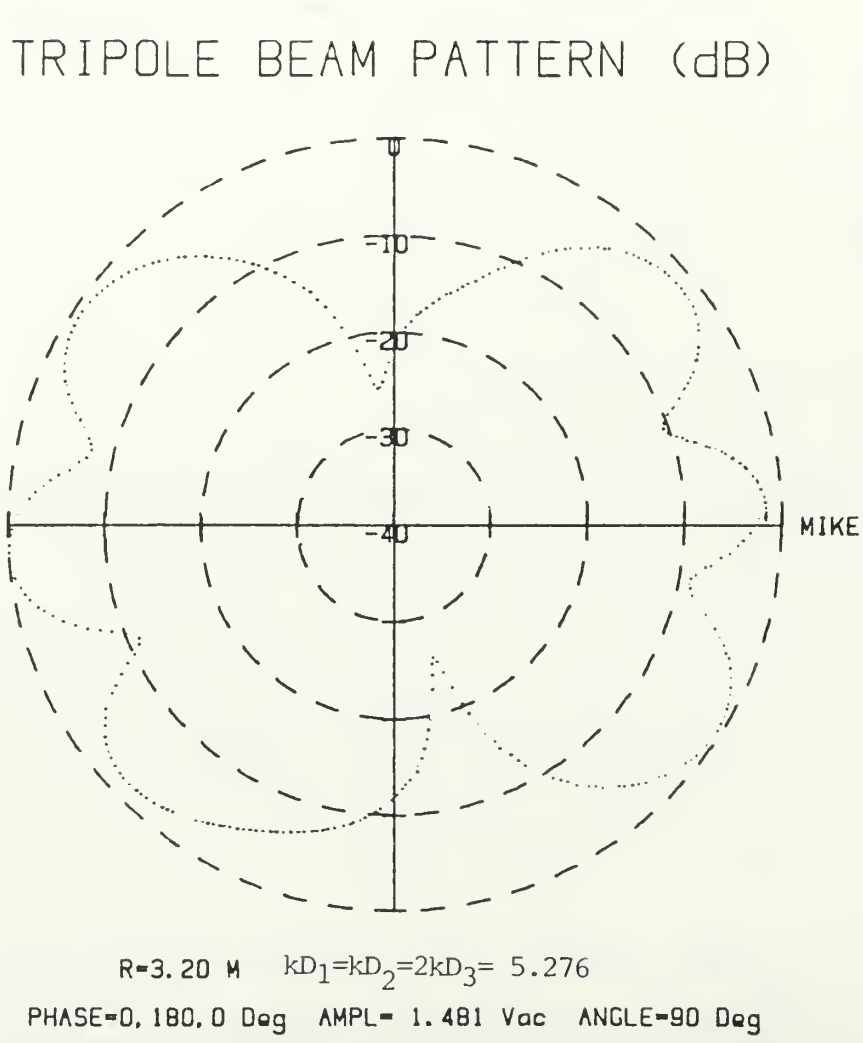

Figure C.7 Beam Pattern for 90^{O} Tilt in Theta (Tripole Isosceles)

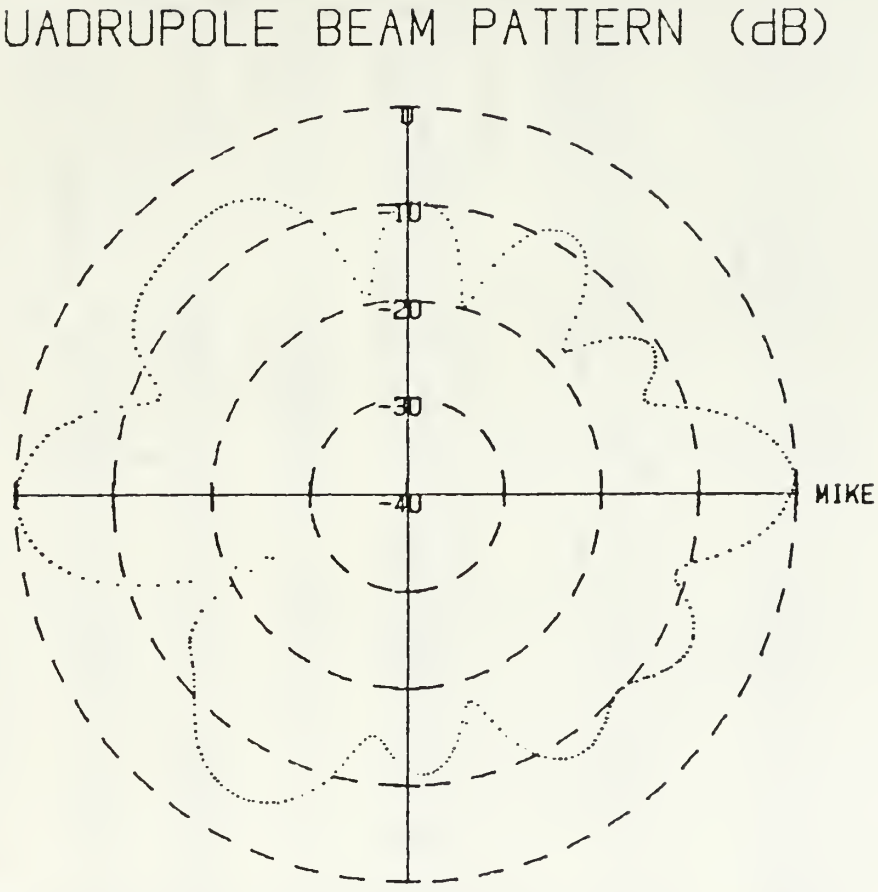

Figure C.8 Beam Pattern for 60° Tilt in Theta (Planar Quadrupole)

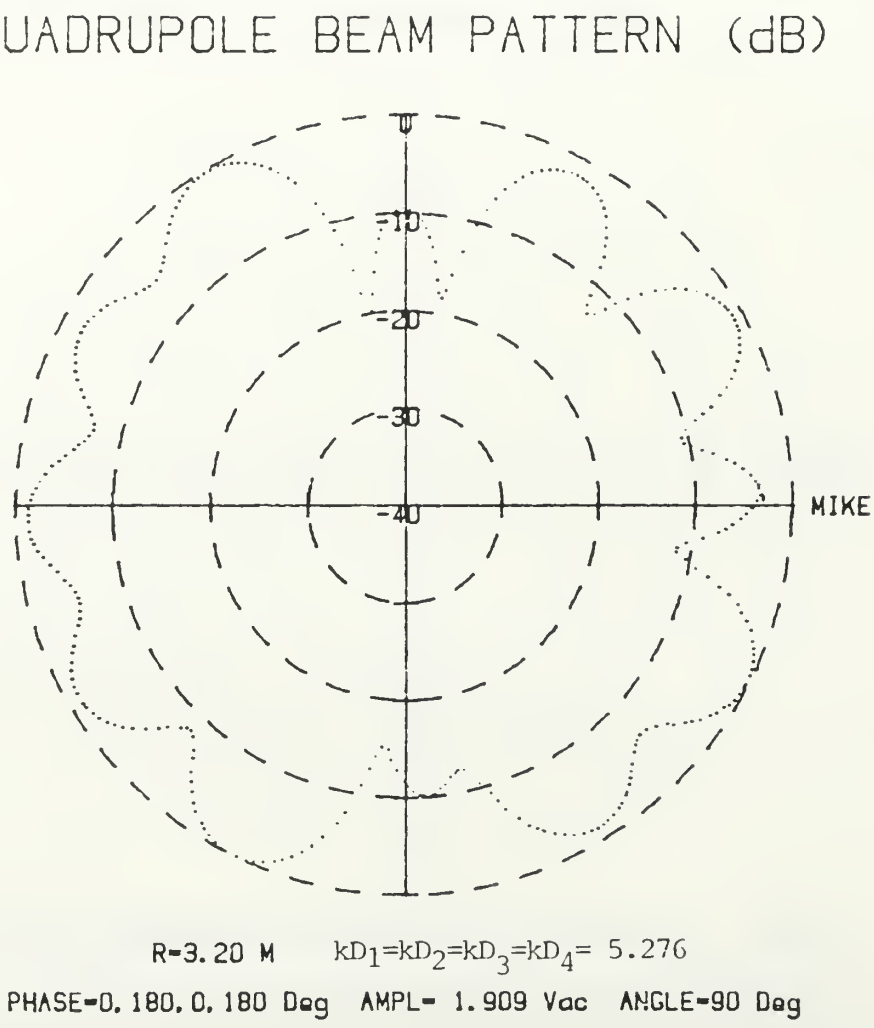

Figure C.9 Beam Pattern for 90^{O} Tilt in Theta (Planar Quadrupole)

LIST OF REFERENCES

1. Park, Y. S., A Study of Directional and Frequency Properties of Shaded and Phased Simple Arrays, pp. 14-20, Master's Thesis, Naval Postgraduate School, Monterey, CA, 1986.

2. Robertson, G. D., Small-Aperture Directional Hydrophones, pp 1-3, IEEE Electronics and Aerospace Systems Convention, Arlington, VA, 24 September 1978.

3. Hughes, W. J., and Thompson, W., "Tilted Directional Response Patterns Formed by Amplitude Weighting and a Single 90 Degree Phase Shift," Journal of the Acoustical Society of America, V. 59, pp. 1040-1045, 1976.

4. Moses, B.O., and Smith, D. A., "Beamforming Experiments with a Cylindrical Array Using Real Shading Coefficients," Journal of the Acoustical Society of America, V. 57(51), p. S12A, 1975.

5. Flanagan, J. L., Johnson, J. D., Zann, R. and Elko, G.W., "Computer-steered Microphone Arrays for Sound Transduction in Large Rooms," Journal of the Acoustical Society of America, V. 78, pp. 1508-1518, 1985.

6. Kinsler, L. E., Frey, A. P., Coppens, A. B., and Sanders, J.V., Fundamentals of Acoustics, pp. 169-172, Wiley, New York, 1982.

7. Olson, H. F., Elements of Acoustical Engineering, pp. 256-259, D. Van Nostrand Co., Inc, New York, 1947.

8. Ziomek, L. J., Underwater Acoustics - A Linear Systems Theory Approach, pp. 145-151, Academic Press, New York, 1985.

9. Deams, S. and Gonzales, J., Two Strategies For Acoustic Localization in Air Using a Compact Sensor, pp. 53-57 Master's Thesis, Naval Postgraduate School, Monterey, CA, 1986

BIBLIOGRAPHY

Collins, R. E., Antennas and Radiowave Propagation, McGraw Hill, New York, 1985.

Collins, R. E., Field Theory of Guided Waves, McGraw-Hill, New York, 1960.

Davids, N., Thurston, E. G., and Muesser, R. E., "The Design of Optimum Directional Acoustic Arrays," Journal of the Acoustical Society of America, V. 24(1), p. 50, 1952.

Drost, C. J., "Near and Forfield of Strip-Shaded Acoustic Radiators," Journal of the Acoustical Society of America, V. 65(3), p. 565, 1979.

Haddow, J. B., "A Novel Formulation for Acoustic Radiation from Dipole (force-like) Sources," 11th International Congress Acoustic, Paris, p. R-27, 1983.

Hasegawa, T., "Calculation of Shading Effect in Near Field by Ring-Function Method," Journal of the Acoustical Society of America, V. 61(2), p. 594, 1977.

Jiotta, J., "Near Field and Far Field of Pulsed Acoustic Radiators," Journal of the Acoustical Society of America, V. 71(4), p. 824, 1982.

Kesner, J. W., "Predicting and Improving Array Beam Patterns," Journal of the Acoustical Society of America, V. 61(51), p. 582A, 1977.

Pritchard, R. L., "Optimum Directivity Patterns for Linear Point Arrays," Journal of the Acoustical Society of America, V. 25(5), p. 870, 1953.

Rhodes, D. R., Synthesis of Planar Antenna Sources, Clarendon Press, Oxford, 1974.

Robertson, G. D., "Small-Aperture Directional Hydrophones," Magnavox Government and Industrial Electronics, IEEE Electronics and Aerospace Systems Convention, 24 Sep 1978.

Silver, S., Microwave Antenna Theory and Design, McGraw-Hill, New York, 1949.

Smith, D. A., "Beam Pattern Control by use of Real Shading Coefficients," Journal of the Acoustical Society of America, V. 57(51), p. 512A, 1975.

Smith, W., Antenna Manual, Editors and Engineers, Ltd., Santa Barbara, CA, 1948.

Steinberg, B. D., Principles of Aperture and Array System Design, John Wiley and Sons, New York, 1976.

Stutzman, W. L. and Thiele, G. A., Antenna Theory and Design, John Wiley and Sons, New York, 1981.

Urick, R. J., Principles of Underwater Sound, McGraw-Hill, New York, 1983.

Wang, H.S.C., "Effectiveness of Optimum Beamforming by Amplitude Shading of Transducer Arrays," Journal of the Acoustical Society of America, V. 57(51), p. 513A, 1975.

Welch, G. B., Wave Propagation and Antennas, D. Van Nostrand Co, Inc., Princeton, 1958.

INITIAL DISTRIBUTION LIST

		No. of Copies
1.	Defense Technical Information Center Cameron Station Alexandria, VA 22304-6145	2
2.	Library, Code 0142 Naval Postgraduate School Monterey, CA 93943-5002	2
3.	Prof. Alan B. Coppens Department of Physics (Code 61Cz) Naval Postgraduate School Monterey, CA 93943	3
4.	LCDR Greg Netzorg Department of Physics (Code 61Nz) Naval Postgraduate School Monterey, CA 93943	1
5.	Prof. S. L. Garrett Department of Physics (Code 61Gx) Naval Postgraduate School Monterey, CA 93943	1
6.	Prof. O. B. Wilson Department of Physics (Code 61Wl) Naval Postgraduate School Monterey, CA 93943	1
7.	Prof. D. L. Walters Department of Physics (Code 61We) Naval Postgraduate School Monterey, CA 93943	2
8.	Prof. S. Baker Department of Physics (Code 61Ba) Naval Postgraduate School Monterey, CA 93943	1
9.	Prof. J. V. Sanders Department of Physics (Code 61Sd) Naval Postgraduate School Monterey, CA 93943	1

10. LCDR John D. Butler 3
c/o Stevens
22 Magnolia Drive
Spring Lake Hts., NJ 07762

11. Mr. & Mrs. Dale Butler 1
1510 Wayside Drive
Texas City, TX 77590

12. Mr. & Mrs. Fred Stevens 1
22 Magnolia Drive
Spring Lake Hts., NJ 07762

13. Major Young Soo Park 2
Dong Jak-Gu Shin Dae Bang - 1 Dong
607 Mu Rin Apt. D-401
Seoul, Korea